NUREG/CR-4267
PNL-5469

Vessel Integrity Simulation Analysis (VISA) Code Sensitivity Study

Prepared by E. P. Simonen, K. I. Johnson, F. A. Simonen

Pacific Northwest Laboratory
Operated by
Battelle Memorial Institute

Prepared for
U.S. Nuclear Regulatory Commission

NUREG/CR-4267
PNL-5469

Vessel Integrity Simulation Analysis (VISA) Code Sensitivity Study

Manuscript Completed: June 1985
Date Published: December 1985

Prepared by
E. P. Simonen, K. I. Johnson, F. A. Simonen

Pacific Northwest Laboratory
Richland, WA 99352

Prepared for
Division of Safety Technology
Office of Nuclear Reactor Regulation
U.S. Nuclear Regulatory Commission
Washington, D.C. 20555
NRC FIN B2510

ABSTRACT

In a study conducted for the Nuclear Regulatory Commission by Pacific Northwest Laboratory, the sensitivity of through-wall crack probability to input distributions was studied. Flaw growth characteristics were evaluated for three pressurized water reactor plants (Oconee 1, Calvert Cliffs 1, and a hypothetical plant similar to H. B. Robinson 2). Three postulated pressurized thermal shock (PTS) transients were considered for each plant. This report describes the results of material and flaw distribution assumptions on calculated conditional failure probabilities for the three reactors under postulated severe PTS transients. The reasons for the predicted sensitivities are evaluated and are related to requirements for defining input distributions for probabilistic failure predictions.

SUMMARY

In a study conducted for the Nuclear Regulatory Commission by Pacific Northwest Laboratory, the sensitivity of through-wall crack probability to assumed input distributions and assumed flaw characteristics was evaluated for three presurized water reactor (PWR) plants and three postulated pressurized thermal shock (PTS) transients for each plant. This report describes the effect of material and flaw distribution assumptions on calculated conditional failure probabilities for Oconee 1, Calvert Cliffs 1, and a hypothetical H. B. Robinson 2. The calculated probabilities are presented as a function of effective full-power years (EFPY) or as a function of reference temperature for the nil ductility transition (RT_{NDT}). The reasons for the predicted sensitivities are evaluated and related to requirements for defining input distributions for use in probabilistic failure predictions.

Probabilistic calculations give an indication of relative failure probabilities for selected conditions of interest. This study has shown how the absolute failure probabilities are affected by specific assumptions made in the calculations. The most critical uncertainty in making probabilistic failure estimates was found to be the lack of knowledge about the flaw depth, length, and position within the vessel wall. Critical review of these flaw assumptions is recommended when evaluating results from failure probability studies. Uncertainties in material property distributions were found to be less significant than were the flaw uncertainties. Simulated parameters for materials properties generally did not deviate from assumed mean values by more than two standard deviations for cases of initiation. Therefore, knowledge of these distributions in the tails beyond two standard deviations is not required for the failure probability calculations. Analyses of initiation events indicated a transition from failures caused by brittle materials and shallow flaws at high failure probabilities to failures caused by ductile materials and deep flaws at low failure probabilities.

Increases in the uncertainty in the copper content and fracture toughness resulted in significant increases in the calculated failure probability. These increases in failure probability were less than one order of magnitude. Comparisons of finite length flaws to infinite flaws, buried flaws to surface flaws, and inspected vessels to noninspected vessels each resulted in about two orders of magnitude decrease in the calculated failure probability. The assumed trend curve for predicting the irradiation shift in the RT_{NDT} was found to have a significant but not dominant influence on the calculated failure probability.

At low fluences, ductile initiation of deep cracks was predicted; whereas at high fluences, brittle initiation of shallow cracks was predicted. Failure probabilities less than 10^{-5} were characterized by cracks deeper than 2.5 in. and by copper contents that were near the assumed mean values. Failure probabilities greater than 10^{-4} were generally characterized by cracks shallower than 1 in.

The copper content was the only material property that sometimes required knowledge of the distribution beyond two standard deviations of the mean. At

intermediate failure probabilities, the average copper content for the simulated initiations exceeded two standard deviations above the mean for a few cases. The simulated fracture toughness values for an initiation event were typically about one standard deviation, and never less than two standard deviations, below the mean.

The assumptions of flaw length, position within the vessel wall, and inspection had strong influences on initiation probabilities and also influenced crack arrest after initiation. Finite length flaws compared to infinite-length flaws required greater material embrittlement to achieve comparable failure probabilities because of pinning constraints at the flaw ends. Buried flaws did not initiate as readily as surface flaws because they had a lesser driving force for initiation and were not as frequently within the near inner-surface embrittled region. When the flaw size distribution was modified to account for in-service inspection, the initiations and hence failures were reduced because the assumed population of flaws was reduced.

CONTENTS

FIGURES

TABLES

TABLES

1.0 INTRODUCTION

Pressurized thermal shock (PTS) is an event that induces thermal stresses in addition to pressure stresses during rapid cooling of a pressurized water reactor (PWR) vessel. At sufficiently low temperatures and high pressures, there may exist a significant probability that a crack in a vessel may propagate through the vessel wall. The probability of through-wall crack propagation is determined by the driving force for crack growth and by the fracture resistance of the vessel wall. The driving force is caused by thermal and pressure stresses; the fracture resistance is a temperature-dependent material property of the vessel wall. Thermal and pressure stresses are a function of the transients in inner-wall temperature and pressure. Fracture resistance is a function of wall temperature, irradiation exposure (i.e., age of the plant), material chemistry, material form (i.e., plate or weld metal) and the initial unirradiated fracture resistance.

Probabilistic fracture mechanics methods are used to estimate conditional failure probabilities given that a particular transient occurs. Distributions in material properties and flaw sizes are input parameters. The Vessel Integrity Simulation Analysis (VISA)[1] and Over-Cooling Accident Probabilistic (OCA-P)[2] codes are Monte Carlo computer codes that have been used to calculate through-wall crack probabilities for the transients of the Integrated Pressurized Thermal Shock (IPTS) program.[3-5] The OCA-P code is being used by Oak Ridge National Laboratory (ORNL) to estimate the integrated risk from postulated transient events. The VISA code is being used by the Pacific Northwest Laboratory[(a)] to evaluate assumptions about input distributions and also the calculational methods of the probabilistic analyses.

This report describes results of VISA sensitivity calculations. Assumptions made in the IPTS through-wall crack probability estimates were evaluated. Three representative severe transients for each of the three plants (Oconee, Calvert Cliffs and H. B. Robinson) were examined. The postulated transients were provided by ORNL and the dominant events in the IPTS study for Oconee and Calvert Cliffs.[3-4] The VISA calculations for H. B. Robinson were made before the IPTS study was completed.[5] Therefore, the transients examined for the hypothetical H. B. Robinson vessel were not the dominant transients reported by ORNL. Each sensitivity was evaluated for irradiation exposures ranging from the early life exposure to the end-of-life plant exposure as expressed in terms of effective full-power years (EFPY). The hypothetical H. B. Robinson vessel was evaluated beyond a realistic end of life to study sensitivities up to reference temperature for the nil ductility transition (RT_{NDT}) values near the PTS screening criteria.[6] Longitudinal flaws were evaluated in each case.

Uncertainty in material properties and flaw assumptions were evaluated. The method of estimating the RT_{NDT} and the uncertainty in estimating the copper and

---

(a) Operated for the U.S. Department of Energy by Battelle Memorial Institute.

nickel contents of vessel welds were evaluated. Uncertainties in crack initiation toughness and crack arrest toughness were also examined. Flaw assumptions, such as the flaw length, initial flaw position within the wall, and inspection effectiveness also were varied in the calculations to evaluate their influence on through-wall crack probability.

2.0 BASES FOR SENSITIVITY CALCULATIONS

2.1 VISA CODE

The Vessel Integrity Simulation Analysis (VISA) code is a Monte Carlo computer simulation of through-wall crack probability given a transient event. The code calculates conditional failure probability based on random selection of parameters from assumed input distributions. For each set of simulated parameters, the driving force for crack propagation is compared to the material resistance for crack propagation. If the driving force is larger than the resistance, the crack is assumed to initiate and propagate through the wall until it either arrests part way through the wall or propagates through the wall. A simulation that results in through-wall propagation is counted as a failure. A simulation that does not predict through-wall propagation is counted as a nonfailure. After a predetermined number of simulations, usually one million, the number of failures is divided by the total number of simulations to obtain the conditional failure probability for the given set of assumptions.

2.2 INPUT DISTRIBUTIONS

Two categories of input distributions were evaluated: material property distributions and flaw distributions.

Fracture resistance is estimated through a series of relationships that describe the influence of weld chemistry and neutron exposure on the expected fracture toughness. Uncertainties in parameters in these relationships result in uncertainty in the final estimate of fracture resistance. The fracture resistance is calculated from knowledge of the material temperature and the material RT_{NDT}, where RT_{NDT} is the nil ductility transition reference temperature. The material RT_{NDT} is calculated from statistical trend equations that express RT_{NDT} as a function of copper content, nickel content, neutron exposure, and the initial unirradiated RT_{NDT}. All material property distributions are assumed to be normal distributions.

The flaw distribution is obtained from evaluations of the probability of occurrence of flaws for a range of depths. In addition to the flaw depth distribution, there is uncertainty in knowing the flaw length and the flaw position. If a weld has been subjected to inspection and repair of flaws after fabrication, then the flaw size distribution has to be modified accordingly.

2.2.1 Material Property Distributions

The copper and nickel content of pressure vessel welds has been determined from weld chemistry studies. In particular, the Babcock and Wilcox (B&W) study[7] indicated expected variations in copper and nickel content within a given weld. A representative standard deviation of copper within a weld was determined to be 0.025% copper. A representative uncertainty based on all welds made from copper-coated electrode wire was 0.065% copper. Therefore, in the present sensitivity study, the effect of weld-specific uncertainty, 0.025%, and the

effect of generic weld uncertainty, 0.065%, on calculated failure probabilities were evaluated.

Nickel uncertainty was investigated by assuming no uncertainty (i.e., no simulation of the nickel distribution) and by assuming an uncertainty of 0.05% that was estimated from the B&W weld chemistry study. Special consideration was given to Calvert Cliffs welds that were made using a three-wire technique in which one wire was pure nickel.[8] In that case, the welder introduced variation in the nickel content by altering the feed rate of the pure nickel wire. Therefore, nickel uncertainty for the Calvert Cliffs sensitivity to nickel was assumed to be either zero or 0.15% nickel.

Fluence uncertainty is caused by uncertainty in the vessel wall dosimetry measurements[9] and by the methods of predicting doses at a weld position given the dosimetry measurement at the surveillance capsule location. A conservative uncertainty of 30% of the expected fluence value was assumed for Oconee, Calvert Cliffs, and H. B. Robinson.

Uncertainty in the initial RT_{NDT} was assumed to be 15°F and its sensitivity on calculated failure probability was not evaluated. The uncertainty was based on the Combustion Engineering study[8] of variation in the initial RT_{NDT}s from weld metal. That study reported a standard deviation of 17°F for the initital RT_{NDT}.

Statistical analyses of the irradiation indexed shift of RT_{NDT} for pressure vessel materials have indicated the dependence of RT_{NDT} shift on copper content, nickel content, and fluence. Two trend curves from statistical analyses were examined in this study. The first, the PTS trend curve, was used in the ORNL analysis of PTS vessel failure probabilities using OCA-P. The second is the weld trend curve. The PTS trend curve is based on a statistical analysis of measured shifts in RT_{NDT} obtained both from PWR plate and PWR weld metal surveillance specimens.[10] The weld trend curve is based on a statistical analysis of measured shifts obtained only from weld metal surveillance specimens for the influence of chemistry[11] and fluence.[12] The weld trend curve has been proposed as Regulation Guide 1.99 Revision 2. The trend curves for RT_{NDT} have the form:

$$RT_{NDT} = RTNDT(0) + CF * FF, \quad (1)$$

where RTNDT(0) is the initial RT_{NDT}, and CF ard FF are the chemistry factor and fluence factor, respectively. For the PTS curve,

$$CF = (-10 * 470 * Cu + 350 * Cu * Ni) \quad (2)$$

and

$$FF = (\text{fluence} / 10^{19})^{0.27} \quad (3)$$

For the weld trend curve,

$$CF = 360 * Cu [(1 + 1.38\ \text{erf}((0.3 * Ni - Cu)/Cu + 1.0)] \quad (4)$$

and

$$FF = (\text{fluence}/10^{19})^{0.28-0.1 \log_{10}(\text{fluence}/10^{19})} \quad (5)$$

Fluence is expressed in units of n/cm^2, $E > 1$ MeV.

Uncertainty in fracture initiation toughness, K_{IC}, and fracture arrest toughness, K_{IA}, was assumed to be either 10% or 20% of the estimated mean value. The 10% value is representative of uncertainty on the lower shelf,[13] while values closer to 20% may be representative of uncertainties in the transition region.

The effect of including an uncertainty in the trend curve correlation was evaluated by simulating a correlation error in addition to simulating copper, fluence, and initial RT_{NDT}. The simulated error was subsequently added (or subtracted) from RT_{NDT} determined as in the standard predictions. The standard deviation in the trend curve correlation was assumed to be 22°F.[10]

2.2.2 Flaw Distributions

The OCTAVIA flaw-size distribution[14] was used to simulate the flaw depth. For the baseline calculations, the flaw is assumed to be infinitely long and located at the inside surface of the vessel. Furthermore, the OCTAVIA distribution does not account for the expected benefits of in-service inspection.

For conservatism and convenience, the flaw length for the standard condition is assumed to be of infinite length in the axial direction. In reality, the flaws have finite lengths and therefore require larger driving force for propagation compared to the infinitely long flaws. A finite flaw is pinned at the ends, which provides resistance to the crack increasing in depth. The dependence of calculated failure probabilities based on finite length flaws was compared to probabilities based on infinitely long flaws. The finite flaw was assumed to have a length to depth ratio of 6:1.

The effect of assuming that flaws are buried and randomly distributed through the thickness of the weld, rather than always at the inner surface, was investigated. There is a larger driving force required for a buried flaw than for a surface flaw of the same depth. Buried flaws are not located in the inner surface region of maximum tensile stress. Also, the inner surface has the lowest toughness due to maximum fluence and minimum temperature. Buried flaws randomly placed within the weld were simulated to compare probabilities based on buried flaws to those on surface flaws. In the case of the buried flaw, the flaw is first allowed to propagate toward the inner surface. The flaw next becomes a surface flaw, which is then allowed to extend toward the outer wall of the vessel. For buried flaws, the flaw depth refers to the distance between the two crack tips.

The flaw size distribution was modified to account for detection during in-service inspection. The inspection was an ultrasonic examination for near-surface cracks. Such an examination would exceed the effectiveness of the

minimum code inspection performed at the time of vessel fabrication. Data from a PNL report to the U.S. Nuclear Regulatory Commission was used to estimate detection probabilities.[15] For conditions of a vessel with a smooth clad surface, the probability of detection of under-clad cracks was taken to be 95% for cracks 0.25 in. or greater in depth. Subsurface or buried flaws were taken to be undetectable if they were more than 1.25 in. below the inner surface of the vessel.

3.0 PLANT-SPECIFIC INPUTS

Simulations were performed for each of the three plants. Hypothetical chemistries and fluences were used for the case of the H. B. Robinson analysis to evaluate sensitivities for conditions near the screening critieria of RT_{NDT} plus two standard deviations equal to 270°F. The hypothetical values for H. B. Robinson in this study are not the same as those assumed in the ORNL study.[5] The critical welds for Oconee 1 and Calvert Cliffs 1 were identified and the properties of the critical welds were used for the simulations. The transient events were selected from the ORNL analysis for each plant.[3-5]

3.1 WELD CHARACTERISTICS

The mean values of critical weld chemistries and fluences are those used in the ORNL reports for Oconee 1 and Calvert Cliffs 1. The plant critical weld numbers and chemistries are shown in Table 1 along with the hypothetical parameters for the case of H. B. Robinson.

The EFPY, fluence, and RT_{NDT} values for the simulations are shown in Table 2. RT_{NDT}'s listed in Table 2 were calculated from the PTS trend curve using a value of 58.8°F for two standard deviations as stated in the PTS Rule. The range of EFPY was selected to produce a range of RT_{NDT} that would approach or exceed the screening criteria as given in the PTS Rule.

Similarly, the pressure and temperature transients for the plant-specific simulations were obtained from ORNL.[3-5] These transients are representative of severe PTS events for the plants. The transients for each plant were as follows: Oconee (TBVG4, MSLB1, and 6A), Calvert Cliffs (2.1, 2.4, and 8.3) and H. B. Robinson (6.6, 6.9, and 8.6).

TABLE 1. Assumed Mean Values for Weld Copper Content, Nickel Content, and Initial RT_{NDT} for Each Plant Evaluated

Plant/Weld	%Copper	%Nickel	RT_{NDT} (0), °F
Oconee 1 SA1430	0.29	0.55	20
Calvert Cliffs 1 2-203	0.21	0.87	-56
H. B. Robinson Hypothetical for material property sensitivity	0.21	0.87	-56
H. B. Robinson Hypothetical for flaw assumption sensitivity	0.19	1.00	-56

TABLE 2. Relationships Among Assumed Fluence Values, Calculated EFPY, and RT_{NDT}

Plant	EFPY	Fluence, 10^{18} n/cm²	RT_{NDT}, °F
Oconee 1	10	3.8	154
	20	7.0	168
	30	10.2	206
	40	13.5	277
Calvert Cliffs 1	10	18.9	184
	20	37.9	222
	30	56.8	247
	40	75.8	267
	50	94.7	283
H. B. Robinson Hypothetical for material property sensitivity		14.6	167
		43.0	224
		98.8	281
		195.0	338
H. B. Robinson Hypothetical for flaw assumption sensitivity		43.0	214
		98.8	268
		195.0	323

3.2 PARAMETERS OF SENSITIVITY ANALYSIS

Several uncertainties were varied in the probabilistic sensitivity calculations. These parameters and uncertainties are shown in Table 3. The sensitivity of failure probability to each was evaluated independently of the others. The table shows the standard uncertainty values assumed for the baseline calculations. The uncertainty values used for each sensitivity examination are also shown. The uncertainties in material properties represent minimum realistic values and maximum realistic values. The flaw parameters are conservative and nonconservative conditions.

TABLE 3. Standard and Sensitivity Values of Selected Parameters

Parameter	Standard Value	Sensitivity Value
Copper standard deviation	0.025 wt%	0.065 wt%
Nickel standard deviation	0.0 wt%	0.05 wt% 0.15 for Cal Cliffs
RT_{NDT} trend curve	PTS	Weld trend curve
Error in RT_{NDT}	None	Error added
K_{IC}/K_{IA} standard deviation	10% of mean	20% of mean
Flaw position	Surface	Buried
Flaw length	Infinite	Finite (6:1 length-to-depth ratio)
Inspection	None	Yes

4.0 RESULTS

The sensitivities to material properties were found to be less important than the sensitivities to flaw assumptions. Increasing the uncertainty in the material property values caused increases in the predicted probabilities that were less than a factor of ten, whereas changes in the flaw assumptions reduced the probabilities by about two orders of magnitude.

Uncertainties in the assumed copper content and the assumed fracture toughness were the most significant uncertainties in the material properties. Increasing the copper standard deviation from 0.025% Cu to 0.065% Cu increased the predicted failure probabilities by factors that were generally less than an order of magnitude. Similarly, increasing the fracture toughness standard deviation from 10% to 20% of its mean value increased the predicted failure probabilities by factors that were less than five. The choice of trend curve for predicting RT_{NDT} resulted in variations in predicted failure probability up to factors of two. Increasing the uncertainty in the nickel content from 0% to 0.05% Ni did not significantly affect the predicted failure probability. However, increasing the uncertainty up to 0.15% Ni did increase the predicted failure probability by factors as large as three.

Flaw length, flaw position, and flaw inspection were assumptions that strongly affected the predicted failure probabilities. Reducing the assumed flaw length, assuming buried flaws instead of surface flaws, and inspection for flaws each reduced the failure probabilities by two orders of magnitude. The flaw length was reduced from an infinite length to one having a length-to-depth ratio of six to one. The flaw position within the vessel was permitted to be at a random depth in contrast to the standard base-case assumption of all flaws being at the inner surface. Lastly, the flaw depth distribution was adjusted to account for flaws that would be repaired after inspection.

4.1 SENSITIVITIES TO MATERIAL PROPERTIES

The sensitivities to material property distributions are shown in Figures 1 through 3 for Oconee 1, Figures 4 through 6 for Calvert Cliffs 1, and Figures 7 through 9 for the H. B. Robinson hypothetical case. The copper, fracture toughness, and trend curve effects on failure probability are shown and compared to the standard baseline conditions. The conditional probabilities of failure are shown in Table 4; the ratios of these probabilities to the standard condition probabilities are shown in Table 5. Increasing the uncertainties in copper content and the fracture toughness increased the probability for failure because larger uncertainty allowed inferior materials properties to be simulated more frequently. The choice of the weld trend curve resulted in lower failure probabilities for Oconee but higher probabilities for Calvert Cliffs and H. B. Robinson compared to calculations based on the PTS trend curve.

The influence of copper uncertainty was dependent on the assumed PTS transient in addition to being dependent the assumed plant. In particular, the copper effects were large for Calvert Cliffs transients 2.1 and 2.4, for which the standard conditional failure probabilities were less than 10^{-4}.

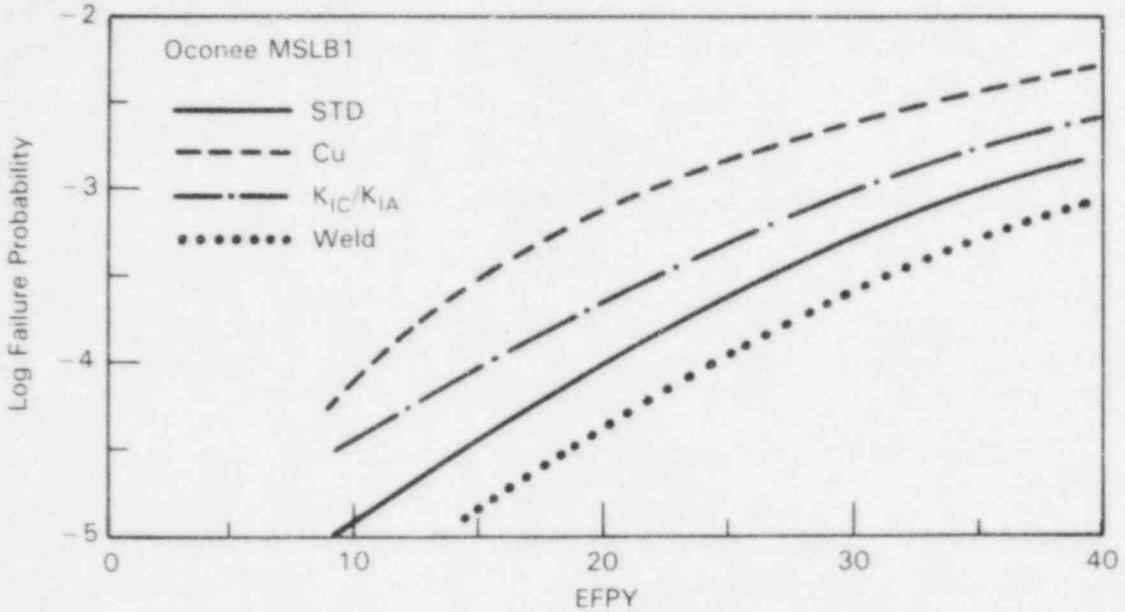

FIGURE 1. Calculated failure probabilities for Oconee 1 Transient MSLB1 for increased copper content and fracture toughness uncertainty compared to the standard uncertainties. Results for the assumed weld trend curve are also shown.

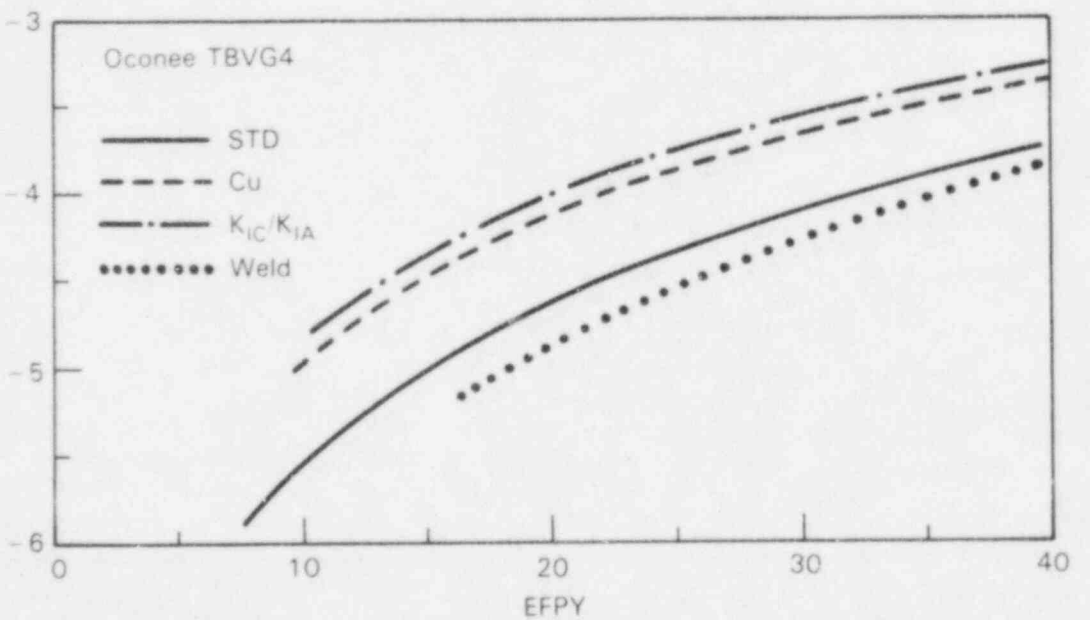

FIGURE 2. Calculated failure probabilities for Oconee 1 Transient TBGV4 for increased copper content and fracture toughness uncertainty compared to the standard uncertainties. Results for the assumed weld trend curve are also shown.

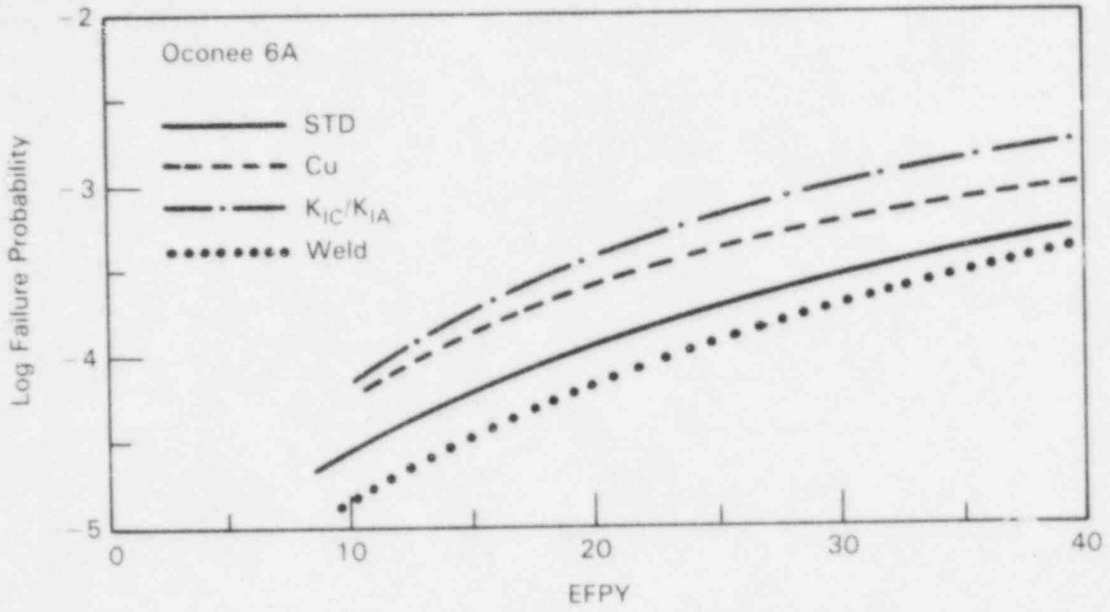

FIGURE 3. Calculated failure probabilities for Oconee 1 Transient 6A for increased copper content and fracture toughness uncertainty compared to the standard uncertainties. Results for the assumed weld trend curve are also shown.

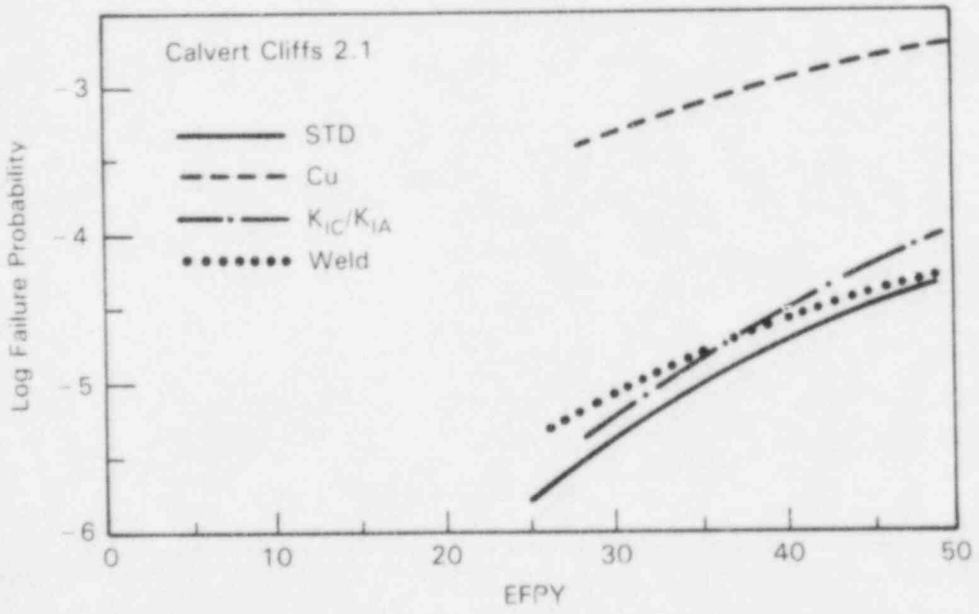

FIGURE 4. Calculated failure probabilities for Calvert Cliffs 1 Transient 2.1 for increased copper content and fracture toughness uncertainty compared to the standard uncertainties. Results for the assumed weld trend curve are also shown.

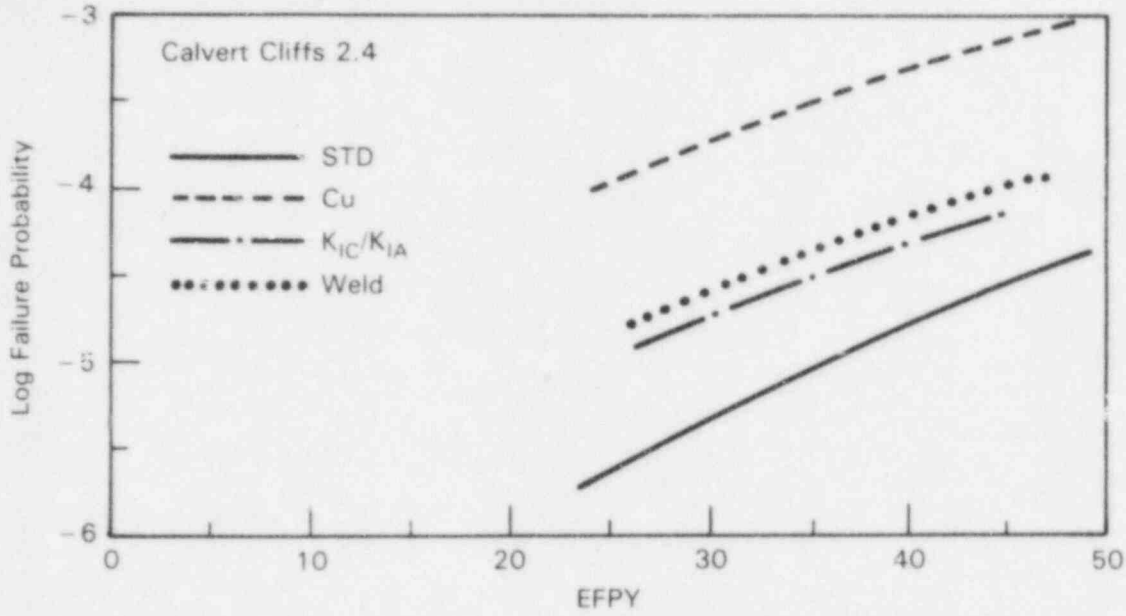

FIGURE 5. Calculated failure probabilities for Calvert Cliffs 1 Transient 2.4 for increased copper content and fracture toughness uncertainty compared to the standard uncertainties. Results for the assumed weld trend curve are also shown.

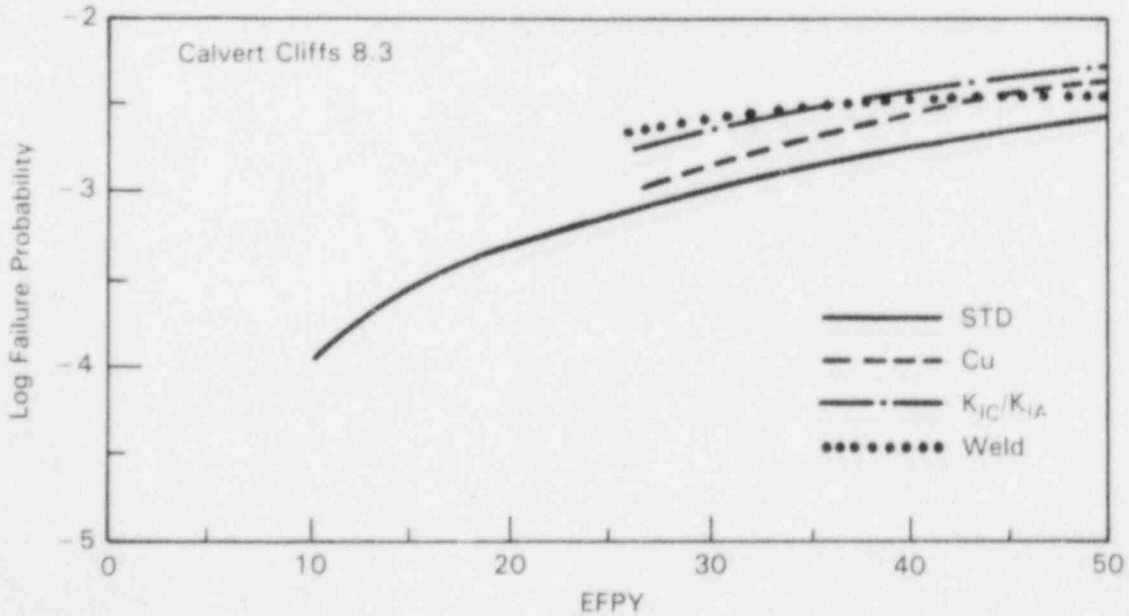

FIGURE 6. Calculated failure probabilities for Calvert Cliffs 1 Transient 8.3 for increased copper content and fracture toughness uncertainty compared to the standard uncertainties. Results for the assumed weld trend are also shown.

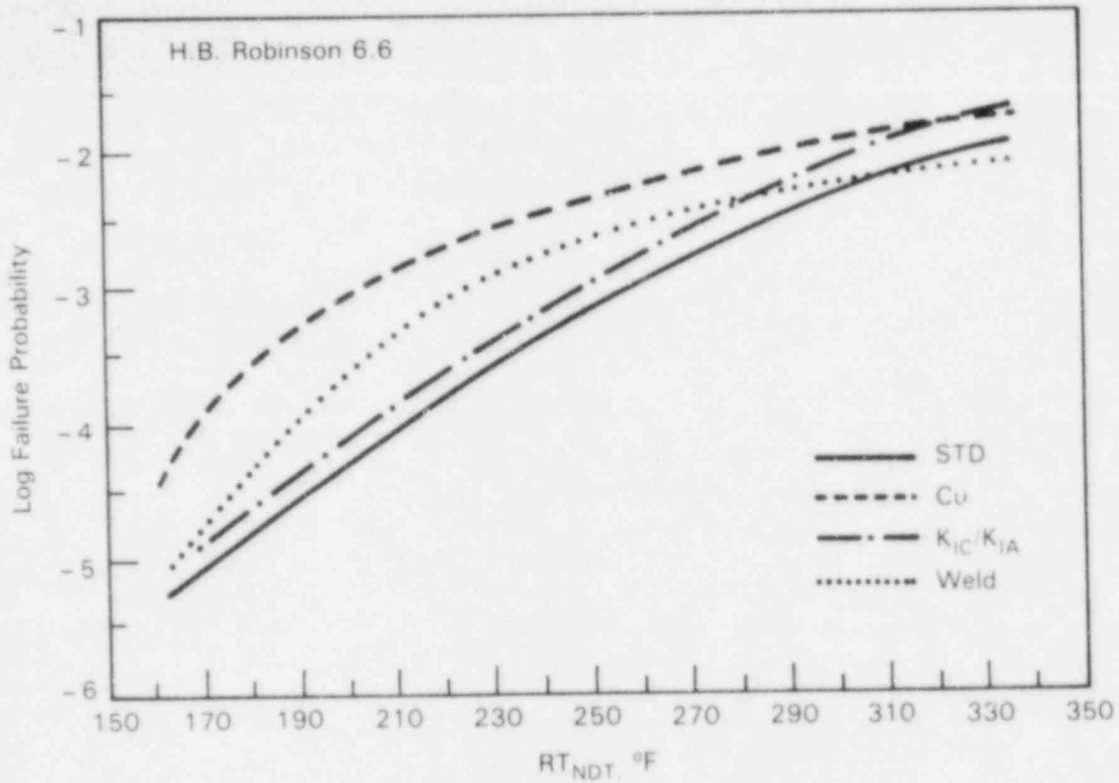

FIGURE 7. Calculated failure probabilities for the hypothetical H. B. Robinson Transient 6.6 for increased copper content and fracture toughness uncertainty compared to the standard uncertainties. Results for the assumed weld trend curve are also shown.

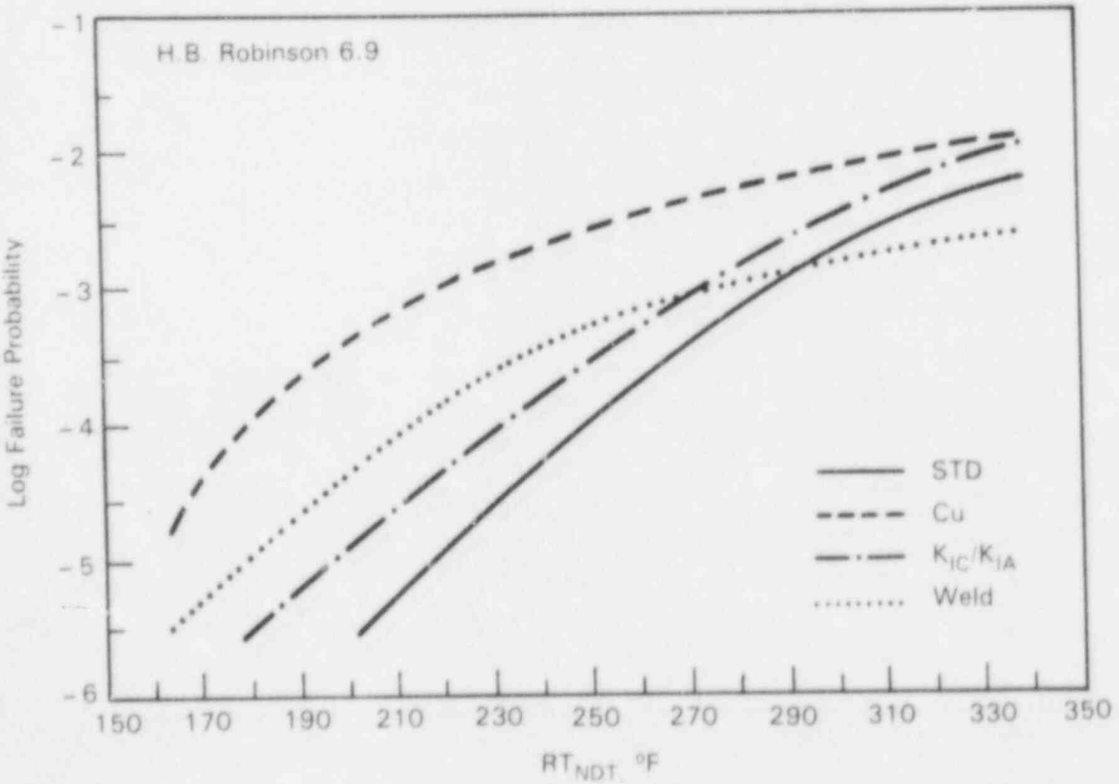

FIGURE 8. Calculated failure probabilities for the hypothetical H. B. Robinson Transient 6.9 increased copper content and fracture toughness uncertainty compared to the standard uncertainties. Results for the assumed weld trend curve are also shown.

TABLE 4. Calculated Failure Probabilities for the Material Property Sensitivity study. All but the correlation ERROR results are plotted in Figures 1 through 9.

PLANT TRANSIENT	FLUENCE N/CM**2	STD	CONDITIONAL FAILURE PROBABILITY CU	NI	KIC	WELD CURVE	CORRELATION ERROR
OCONEE	3.7E+18	2.8E-05	8.0E-05	3.7E-05	4.0E-05	3.0E-05	3.9E-05
MSLB1	7.0E+18	9.2E-05	8.4E-04	1.0E-04	1.7E-04	4.2E-05	1.6E-04
	1.0E+19	5.2E-04	2.6E-03	5.4E-04	1.0E-03	2.4E-04	7.5E-04
	1.4E+19	1.4E-03	5.0E-03	1.5E-03	3.4E-03	9.0E-04	1.8E-03
OCONEE	3.7E+18		1.3E-05	3.8E-06	1.5E-05		1.0E-05
TBVG4	7.0E+18	2.5E-05	9.3E-05	2.4E-05	7.6E-05	1.4E-05	3.5E-05
	1.0E+19	8.0E-05	2.4E-04	7.5E-05	2.7E-04	5.0E-05	9.9E-05
	1.4E+19	1.9E-04	4.6E-04	1.7E-04	5.8E-04	1.5E-04	2.5E-04
OCONEE	3.7E+18	3.0E-05	6.3E-05	2.3E-05	6.7E-05	1.0E-05	3.9E-05
6A	7.0E+18	1.1E-04	2.8E-04	1.1E-04	3.7E-04	6.6E-05	1.6E-04
	1.0E+19	2.6E-04	6.3E-04	2.8E-04	9.8E-04	2.2E-04	3.9E-04
	1.4E+19	5.6E-04	1.0E-03	5.7E-04	1.8E-03	4.7E-04	7.5E-04
CAL CL	1.9E+19	2.0E-06					3.0E-06
2.1	3.8E+19	2.0E-06					3.0E-06
	5.7E+19	4.0E-06	5.0E-04	8.0E-06	6.0E-06	1.0E-05	3.0E-06
	7.6E+19	1.7E-05	1.1E-03	3.3E-05	3.1E-05	2.3E-05	7.8E-06
	9.5E+19	4.6E-05	1.9E-03	1.0E-04	1.0E-04	5.7E-05	4.3E-05
CAL CL	1.9E+19	3.0E-06					3.0E-06
2.4	3.8E+19	3.0E-06					3.0E-06
	5.7E+19	4.5E-06	1.9E-04	1.4E-05	1.9E-05	2.7E-05	1.2E-06
	7.6E+19	1.6E-05	5.1E-04	3.3E-05	4.7E-05	8.0E-05	2.7E-05
	9.5E+19	4.5E-05	1.0E-03	8.6E-05	1.5E-04	1.1E-04	5.8E-05
CAL CL	1.9E+19	9.6E-05					1.3E-04
8.3	3.8E+19	5.1E-04					5.7E-04
	5.7E+19	9.7E-04	1.1E-03	1.2E-03	2.3E-03	2.8E-03	1.1E-03
	7.6E+19	1.8E-03	2.7E-03	1.8E-03	3.6E-03	3.1E-03	2.0E-03
	9.5E+19	2.3E-03	4.2E-03	2.4E-03	5.1E-03	3.5E-03	2.4E-03
HBR	1.5E+19	9.0E-06	7.6E-05	9.0E-06	9.0E-06	1.4E-05	
6.6	4.3E+19	1.3E-04	2.2E-03	1.4E-04	2.9E-04	1.1E-03	
	9.9E+19	2.5E-03	9.8E-03	2.4E-03	4.4E-03	4.3E-03	
	2.0E+20	1.3E-02	1.8E-02	1.3E-02	2.2E-02	7.3E-03	

TABLE 4. (continued)

HBR	1.5E+19	4.0E-06	2.5E-05	4.0E-06	5.0E-06	4.0E-06
6.9	4.3E+19	1.7E-05	1.2E-03	1.8E-05	4.9E-05	1.6E-04
	9.9E+19	9.1E-04	5.8E-03	9.7E-04	1.8E-03	1.4E-03
	2.0E+20	5.8E-03	1.3E-02	5.9E-03	1.0E-02	2.2E-03
HBR	1.5E+19	6.0E-06	9.5E-05	6.0E-06	6.0E-06	1.5E-05
8.6	4.3E+19	1.5E-04	2.4E-03	1.6E-04	3.4E-04	1.6E-03
	9.9E+19	2.7E-03	9.5E-03	2.7E-03	4.3E-03	4.4E-03
	2.0E+20	1.3E-02	1.9E-02	1.4E-02	2.1E-02	8.7E-03

The copper effect was small, nowever, for the Calvert Cliffs transient 8.3, in which case the failure probabilities for the standard conditions were much greater than 10^{-4}. The three transients for Oconee and H. B. Robinson all showed approximately the same magnitude of enhanced probability caused by assuming a large standard deviation in copper content compared to a small standard deviation in copper content. The magnitude of the copper standard deviation effect was not strongly dependent on the assumed irradiation fluence, i.e., EFPY.

The effect of the nickel standard deviation on calculated failure probability was much smaller than that for copper, as seen in Tables 4 and 5. Increasing the nickel standard deviation from 0% to 0.05% Ni for Oconee and H. B. Robinson resulted in no significant change in the calculated probabilities. However, for Calvert Cliffs, increasing the nickel standard deviation from 0% to 0.15% Ni increased the failure probability by factors as great as three. A larger uncertainty was examined for Calvert Cliffs because of the pure nickel wire used in the welding procedure.

Increasing the assumed standard deviation in fracture toughness, K_{IC}, from 10% to 20% of its mean value resulted in higher failure probabilities. The fracture toughness uncertainty had an effect that was similar to but smaller than the copper uncertainty effect. Typical increases in failure probability are shown in Table 5 and range from no increase for H. B. Robinson transient 8.6 at a fluence of 1.5×10^{19} n/cm² to an increase by a factor of 4.2 for Calvert Cliffs transient 2.4 at a fluence of 5.7×10^{19} n/cm².

In addition to assumed material characteristics, the calculated failure probability is dependent on the method of calculating the irradiation-shifted RT_{NDT}. Calculated failure probabilities for two choices of trend curve are shown in Figures 1 through 9. The weld trend curve resulted in lower failure probabilities for Oconee conditions and higher failure probabilities for Calvert Cliffs conditions compared to the PTS (standard) trend curve. For RT_{NDT} values below 270°F, the H. B. Robinson probabilities were higher for the weld trend curve compared to the PTS trend curve. The trend curve choice had the largest influence of one order of magnitude on failure probability for H. B. Robinson. For Oconee, the trend curve choice generally did not change the predicted failure probability by more than a factor of two.

TABLE 5. Ratios of the Calculated Failure Probabilities for the Material Property Sensitivity Cases to the Appropriate Standard Case

PLANT TRANSIENT	FLUENCE N/CM^2	STD FAILURE PROB	SENSITIVITY CASE/STANDARD CASE CU	NI	KIC	WELD CURVE	CORRELATION ERROR
OCONEE	3.7E+18	2.80E-05	2.9	1.3	1.4	1.1	1.4
MSLB1	7.0E+18	9.20E-05	9.1	1.1	1.8	0.46	1.8
	1.0E+19	5.20E-04	4.9	1	1.9	0.45	1.4
	1.4E+19	1.40E-03	3.5	1	1.7	0.62	1.2
OCONEE	3.7E+18						
TBVC4	7.0E+18	2.50E-05	3.7	0.95	3.1	0.56	1.4
	1.0E+19	8.00E-05	3	0.94	3.3	0.63	1.2
	1.4E+19	1.90E-04	2.4	0.91	3.1	0.82	1.3
OCONEE	3.7E+18	3.00E-05	2.1	0.75	2.2	0.33	1.3
6A	7.0E+18	1.10E-04	2.5	1	3.3	0.59	1.4
	1.0E+19	2.60E-04	2.4	1.1	3.7	0.83	1.5
	1.4E+19	5.60E-04	1.8	1	3.2	0.84	1.4
CAL CL	1.9E+19	3.00E-06					
2.1	3.8E+19	2.00E-06					
	5.7E+19	4.80E-06	120	2	1.5	2.5	0.75
	7.6E+19	1.70E-05	64	1.9	1.8	1.4	0.46
	9.5E+19	4.60E-05	40	2.2	2.3	1.2	0.93
CAL CL	1.9E+19	3.00E-06					
2.4	3.8E+19	3.00E-06					
	5.7E+19	4.50E-06	42	3.1	4.2	6	0.27
	7.6E+19	1.60E-05	32	2.1	3	5	1.7
	9.5E+19	4.50E-05	22	1.9	3.2	2.4	1.3
CAL CL	1.9E+19	9.60E-05					
8.3	3.8E+19	5.20E-04					
	5.7E+19	9.70E-04	1.2	1.2	2.3	2.9	1.1
	7.6E+19	1.80E-03	1.6	1	2.1	1.8	1.2
	9.5E+19	2.30E-03	1.6	0.9	1.9	1.3	0.92
HBR	1.5E+19	9.00E-06	8.4	1	1	1.6	
6.6	4.3E+19	1.30E-04	17	1.1	2.3	8.3	
	9.9E+19	2.50E-03	3.9	0.97	1.8	1.7	
	2.0E+20	1.30E-02	1.4	0.95	1.6	0.56	
HBR	1.5E+19	4.00E-06	6.3	1	1.3	1	
6.9	4.3E+19	1.70E-05	70	1.1	2.9	9.6	
	9.9E+19	9.10E-04	5.5	1.1	2	1.5	
	2.0E+20	5.80E-03	2.2	1	1.8	0.39	
HBR	1.5E+19	6.00E-06	16	1	1	2.5	
8.6	4.3E+19	1.50E-04	16	1.1	2.4	11	
	9.9E+19	2.70E-03	3.5	1	1.6	1.6	
	2.0E+20	1.30E-02	1.5	1.1	1.6	0.7	

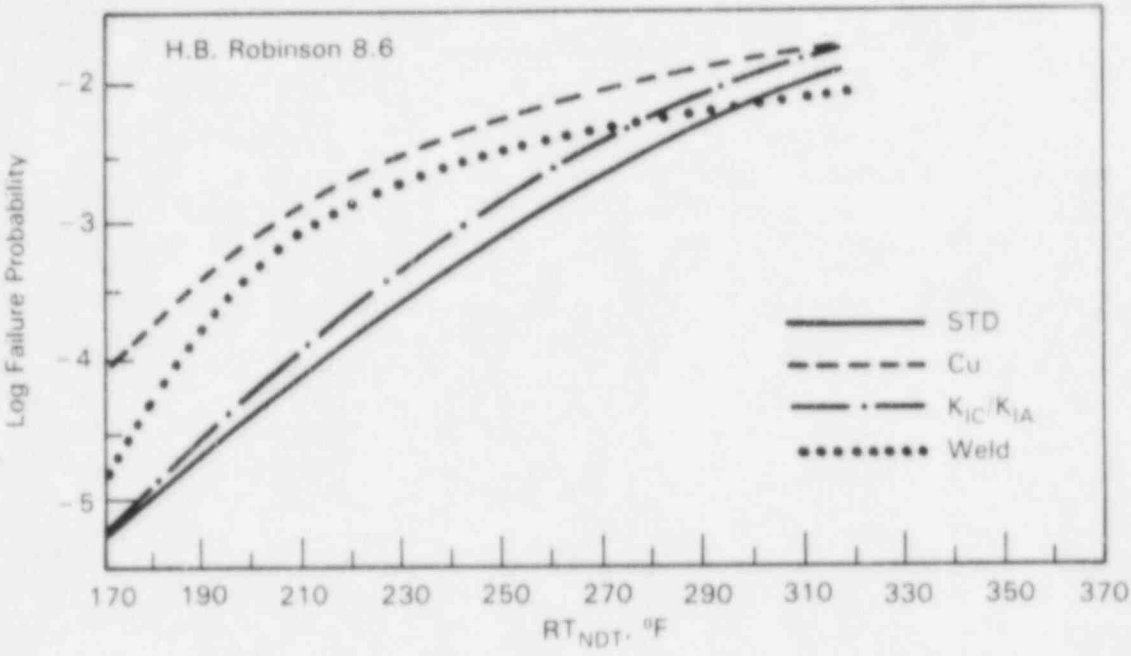

FIGURE 9. Calculated failure probabilities for the hypothetical H. B. Robinson Transient 8.6 for increased copper content and fracture toughness uncertainty compared to the standard uncertainties. Results for the assumed weld trend curve are also shown.

Adding uncertainty to the RT_{NDT} prediction did not significantly increase the calculated failure probabilities. Typically, adding uncertainty to the trend curve correlation increased the failure probability by less than 50% as seen in Tables 4 and 5.

4.2 ANALYSIS OF SIMULATED VALUES FOR INITIATION

Uncertainties in copper content and fracture toughness were evaluated in relation to flaw depth and relative ductility for the simulated initiation events. The evaluation indicated that simulated copper contents for initiations were usually less than two standard deviations above the specified mean values. Simulated fracture toughness values were generally one standard deviation below the specified average values. High failure probabilities were

associated with initiations dominated by brittle initiation of shallow flaws, whereas low failure probabilities were associated with initiations dominated by ductile initiation of deep flaws.

Parametric trends as a function of calculated failure probability for each of the three plants are shown in Figures 10 through 12 and Tables 6 through 8. The data plotted in Figures 10 through 12 include failure probabilities calculated for the standard, copper, and K_{IC} sensitivity conditions for each plant. The copper content and fracture toughness values are referenced to the assumed mean values and normalized by the assumed standard deviation. With increasing failure probability, the average simulated initiation had a smaller flaw depth and a lower value of $T\text{-}RT_{NDT}$. With increasing failure probability, the average simulated copper content was low at the extremes, i.e., low and high probabilities, but high at intermediate failure probabilities. The simulated fracture toughness values were not strongly dependent on the failure probability.

The simulated copper contents for initiation were high at intermediate failure probabilities because the flaws were shallow enough to be affected by irradiation and because failures occurred in the transition region of the fracture toughness curve where RT_{NDT} sensitivities are important. For flaws deeper than 2.5 in., the flaw tip is beyond the zone of significant irradiation damage and therefore is not strongly influenced by the simulated copper content. Failure probabilities less than 10^{-5} were of a ductile type and were associated with flaw depths greater than 2.5 in., $T\text{-}RT_{NDT}$ values greater than 200°F, and copper contents less than one standard deviation above the mean value. Failure probabilities greater than 10^{-5} and less than 10^{-3} were associated with copper contents near to or greater than two standard deviations above the mean value. For H. B. Robinson, Figure 12, a decrease in simulated copper content was evident with an increase in failure probability above 10^{-3}. This indicates that for very high failure probabilities, the failures occurred on the lower shelf for K_{IC}. On the lower shelf, the fracture toughness is insensitive to the RT_{NDT} and hence the assumed copper content. Therefore, the simulated copper contents for initiation should approach the mean copper content at high failure probabilities on the lower shelf.

The Oconee calculations did not show high simulated copper contents because the assumed mean content was high, 0.29%, compared to Calvert Cliffs, 0.21%, and H. B. Robinson, 0.21%. When the assumed mean value was low, the simulated copper contents were high relative to the assumed mean value. In addition, the sensitivity to copper uncertainty was affected by the VISA code assumption that the copper content could not exceed 0.4% Cu. For the assumed high uncertainty in copper content, the mean plus two standard deviations, 0.13%, was 0.42% and was above the 0.4% cutoff. Therefore, the average simulated copper content for Oconee was restricted by the assumed upper limit for copper content.

The simulated fracture toughness values for initiation showed a weak dependence on the magnitude of calculated failure probability. The average toughness values were about one standard deviation below the assumed mean values as seen in Figures 10 through 12. The lowest simulated toughness values were for the Oconee transient, but even for that case, the average values never were less

than two standard deviations below the assumed mean value. The reason for the lack of dependence of the fracture toughness uncertainty on the calculations is that the fracture toughness distribution influenced ductile failures at low fluences, as well as brittle failures at high fluences. Therefore, the sensitivity of failure probability to fracture toughness uncertainty at low probabilities was similar to that at high failure probabilities.

4.3 FLAW ASSUMPTIONS

Assumptions of flaw length, position and inspection strongly affected the calculated failure probability as shown in Tables 9 and 10 and in Figures 13 through 17. Finite-length flaws, buried flaws, and inspection caused one to two orders of magnitude decrease in the probabilities compared to assumptions of long, surface flaws and no in-service inspection. Of the three flaw assumptions in-service inspection had the least influence on the predictions. The predicted failure probabilities often approached 10^{-6}, which is the lower limit of the VISA calculation for one million simulations. Therefore, some of the apparent variations that are evident in the flaw assumption sensitivities are caused by the relatively poor statistical confidences for low-probability calculations.

The assumptions of finite length flaws, buried flaws, and in-service inspection caused decreases in the calculated failure probability because flaw initiation was less frequent. Pinning at the ends of finite flaws decreased the stress intensity factor for initiation at the point of maximum flaw depth. Buried flaws had a reduced probability of being within the brittle inner part of the vessel wall and hence were less susceptible to initiation. Buried flaws also have lower values of stress intensity factor and hence most often did not propagate through to the outer wall. In-service inspection decreased the number of flaws and hence decreased the number of flaws that could initiate.

The assumed finite length of the flaw resulted in pinning restraint that inhibited initiation at the point of maximum depth. Once a finite length flaw initiated, its length was extended to a long flaw and subsequent propagation was predicted in the same manner as a long flaw.

Reduced failure probabilities for buried flaws compared to surface flaws were caused by a reduction in the number of flaws present near the brittle inner surface and by a reduced driving force for propagation. The assumed flaw position had a minor influence on arrest, but a major influence on flaw initiation. The VISA code assumes that the buried flaw first extends to the inner wall. The resulting surface flaw then propagates toward the outer wall. The outward propagation was calculated in the same manner as for the surface flaw of the standard reference case; therefore, no significant differences in the arrest frequency are expected once the flaw initiates. The average size of initiated flaw was increased by the buried flaw assumption for the Calvert Cliffs and Oconee calculations. The average depth of an initiated flaw was not significantly affected by the buried flaw assumption for H. B. Robinson.

The assumption of in-service inspection and repair caused a decrease in the flaw initiation frequency and an increase in the fraction of initiations that

arrested. Inspection generally reduced the average simulated flaw depth for the initiation as calculated for H. B. Robinson. If the flaw depth was shallow for noninspection, as for Calvert Cliffs, inspection had little effect on the average simulated flaw depth.

The high average simulated copper contents that were observed for the standard conditions were not evident for the cases of modified flaw assumptions. In particular, the Calvert Cliffs and the H. B. Robinson simulated copper contents were about one standard deviation lower for the finite flaw, buried flaw, and in-service inspection than for the standard case. The average simulated copper content for Oconee was not sensitive to the flaw assumptions because the simulated copper contents were moderately above the mean even for the standard conditions.

TABLE 6. Average Simulated Parameters for Initiation for Oconee 1 Conditions. The copper content and fracture toughness values are referenced to the assumed mean values and normalized by the assumed standard deviation. Also shown are the calculated initiation and failure probabilities for each condition.

SENSITIVITY TRANSIENT	FLUENCE N/CM**2	FAILURE PROB	INITIATION PROB	SIMULATED COPPER NORMALIZED	SIMULATED KIC NORMALIZED	SIMULATED DEPTH IN	SIMULATED T-RTNDT F
STD	6.99E+18	2.50E-05	2.50E-05	1.05	-1.31	1.42	53
TBVG4	1.02E+19	8.00E-05	8.00E-05	1.31	-1.11	1.06	6
	1.35E+19	1.87E-04	1.87E-04	1.03	-1.02	1.04	0
CU	3.74E+18	1.25E-05	1.25E-05	0.88	-1.35	1.78	116
TBVG4	6.99E+18	9.25E-05	9.25E-05	1.20	-1.28	1.01	4
	1.02E+19	2.43E-04	2.43E-04	1.19	-1.17	0.90	-15
	1.35E+19	4.58E-04	4.60E-04	1.03	-1.15	0.84	-25
KIC	3.74E+18	1.50E-05	3.13E-05	0.78	-1.79	1.34	88
TBVG4	6.99E+18	7.63E-05	1.49E-04	0.93	-1.76	0.89	26
	1.02E+19	2.65E-04	3.95E-04	0.88	-1.68	0.78	2
	1.35E+19	5.83E-04	7.75E-04	0.75	-1.62	0.65	-10
STD	3.74E+18	3.00E-05	3.00E-05	0.90	-1.10	1.52	78
6A	6.99E+18	1.12E-04	1.12E-04	0.88	-1.10	1.20	22
	1.02E+19	2.62E-04	2.64E-04	0.81	-1.01	1.05	4
	1.35E+19	5.58E-04	5.58E-04	0.64	-1.33	0.98	-10
FINITE	1.02E+19	1.00E-06	1.00E-06	1.84		2.00	5
FLAW	1.35E+19	8.00E-06	8.00E-06	1.64		1.31	-39
6A							
BURIED	3.74E+18	0.00E+00	2.00E-06	1.48		1.50	43
FLAW	6.99E+18	3.00E-06	5.00E-06	0.84		1.75	30
6A	1.02E+19	7.00E-06	9.00E-06	0.88		1.44	12
	1.35E+19	9.00E-06	1.40E-05	0.76		1.38	12
INSERVICE	3.74E+18	0.00E+00	2.00E-06	0.40		1.00	45
INSPECTION	6.99E+18	3.00E-06	1.50E-05	0.52		0.93	9
6A	1.02E+19	8.00E-06	3.60E-05	0.52		0.78	-3
	1.35E+19	1.22E-05	5.54E-05	0.44		0.74	-13

TABLE 7. Average Simulated Parameters for Initiation for Calvert Cliffs 1 Conditions. The copper content and fracture thoughness values are referenced to the assumed mean values and normalized by the assumed standard deviation. Also shown are the calculated initiation and failure probabilities for each condition.

SENSITIVITY TRANSIENT	FLUENCE N/CM**2	FAILURE PROB	INITIATION PROB	SIMULATED COPPER NORMALIZED	SIMULATED KIC NORMALIZED	SIMULATED DEPTH IN	SIMULATED T-RTNDT F
STD	1.89E+19	3.00E-06	3.00E-06	0.12	-1.04	3.50	226
2.4	3.79E+19	3.00E-06	3.00E-06	0.12	-1.04	3.50	239
	5.68E+19	4.50E-06	4.50E-06	0.88	-1.13	2.88	163
	7.58E+19	1.60E-05	1.60E-05	1.88	-1.16	1.30	14
	9.47E+19	4.50E-05	5.00E-05	1.72	-1.29	0.99	-16
CU	5.68E+19	1.89E-04	1.89E-04	2.11	-0.84	0.64	-87
2.4	7.58E+19	5.06E-04	5.06E-04	1.95	-0.84	0.49	-109
	9.47E+19	1.01E-03	1.01E-03	1.91	-0.83	0.47	-127
KIC	5.68E+19	1.98E-05	2.00E-05	2.04	-1.56	1.81	13
2.4	7.58E+19	4.73E-05	5.37E-05	1.96	-0.42	0.76	-15
	9.47E+19	1.45E-04	1.48E-04	1.56	-0.42	0.75	-27
STD	1.89E+19	9.62E-05	9.82E-05	0.92	-1.04	1.14	-7
8.3	3.79E+19	5.20E-04	5.20E-04	1.04	-0.95	0.73	-59
	5.68E+19	9.66E-04	9.66E-04	1.08	-1.01	0.60	-90
	7.58E+19	1.75E-03	1.75E-03	0.96	-0.59	0.67	-102
	9.47E+19	2.26E-03	2.26E-03	0.80	-0.63	0.68	-110
FINITE	1.89E+19	1.08E-06	1.50E-05	0.84		1.87	-2
FLAW	3.79E+19	6.66E-06	6.66E-05	0.68		1.58	-37
8.3	5.68E+19	2.01E-06	1.25E-04	0.64		1.40	-68
	7.58E+19	8.76E-05	2.74E-04	0.64		1.25	-84
	9.47E+19	1.23E-04	3.24E-04	0.60		1.22	-100
BURIED	1.89E+19	2.00E-06	3.00E-04	1.16		2.00	23
FLAW	3.79E+19	1.00E-05	1.30E-05	0.92		1.44	28
8.3	5.68E+19	1.80E-05	2.50E-05	0.76		1.43	-49
	7.58E+19	2.70E-05	3.80E-05	0.60		1.24	-70
	9.47E+19	3.80E-05	4.30E-05	0.64		1.23	-83
INSERVICE	1.89E+19	2.00E-06	9.00E-06	0.72		1.06	-6
INSPECTION	3.79E+19	1.50E-05	4.30E-05	0.64		0.77	-45
8.3	5.68E+19	3.41E-05	8.98E-05	0.68		0.61	-78
	7.58E+19	7.91E-05	1.24E-04	0.64		0.56	-98
	9.47E+19	9.31E-05	1.55E-04	0.68		0.52	-114

TABLE 8. Average Simulated Parameters for Initiation for the Hypothetical H. B. Robinson Conditions. The copper content and fracture toughness values are referenced to the assumed mean values and normalized by the assumed standard deviation. Also shown are the calculated initiation and failure probabilities for each condition.

SENSITIVITY TRANSIENT	FLUENCE N/CM**2	FAILURE PROB	INITIATION PROB	SIMULATED COPPER NORMALIZED	SIMULATED KIC NORMALIZED	SIMULATED DEPTH IN	SIMULATED T-RTNDT F
STD	1.46E+19	4.00E-06	4.00E-06	-0.04	-0.01	3.44	377
6.9	4.30E+19	1.70E-05	1.70E-05	1.60	-0.82	1.56	81
	9.88E+19	9.13E-04	9.13E-04	1.60	-0.68	1.19	-7
	1.95E+20	5.78E-03	5.78E-03	1.08	-0.64	1.21	-28
CU	1.46E+19	2.50E-05	2.50E-05	2.17	-0.74	1.26	49
6.9	4.30E+19	1.20E-03	1.20E-03	1.97	-0.51	1.11	-24
	9.88E+19	4.99E-03	4.99E-03	1.58	-0.56	0.63	-85
	1.95E+20	1.27E-02	1.27E-02	1.17	-0.43	0.51	-112
KIC	1.46E+19	5.00E-06	5.00E-06	-0.28	0.06	3.50	332
6.9	4.30E+19	4.90E-05	5.22E-05	1.88	-1.04	2.15	56
	9.88E+19	1.82E-03	1.82E-03	1.40	-0.77	2.01	29
	1.95E+20	1.02E-02	1.02E-02	0.84	-0.81	1.41	-25
FINITE	4.30E+19	0.00E+00	1.00E-06	1.32		2.00	77
FLAW	9.88E+19	1.00E-06	2.30E-05	1.40		1.42	15
6.9	1.95E+20	2.36E-04	2.36E-04	1.28		0.99	-48
BURIED	4.30E+19	1.00E-06	2.00E-06	1.64		1.75	121
FLAW	9.88E+19	3.00E-06	1.90E-05	1.28		0.93	15
6.9	1.95E+20	5.57E-05	7.53E-05	1.00		0.95	-25
INSERVICE	4.30E+19	0.00E+00	5.00E-06	1.68		0.80	43
INSPECTION	9.88E+19	2.01E-05	9.14E-05	1.16		0.71	5
6.9	1.95E+20	2.03E-04	5.09E-04	1.20		0.45	-67

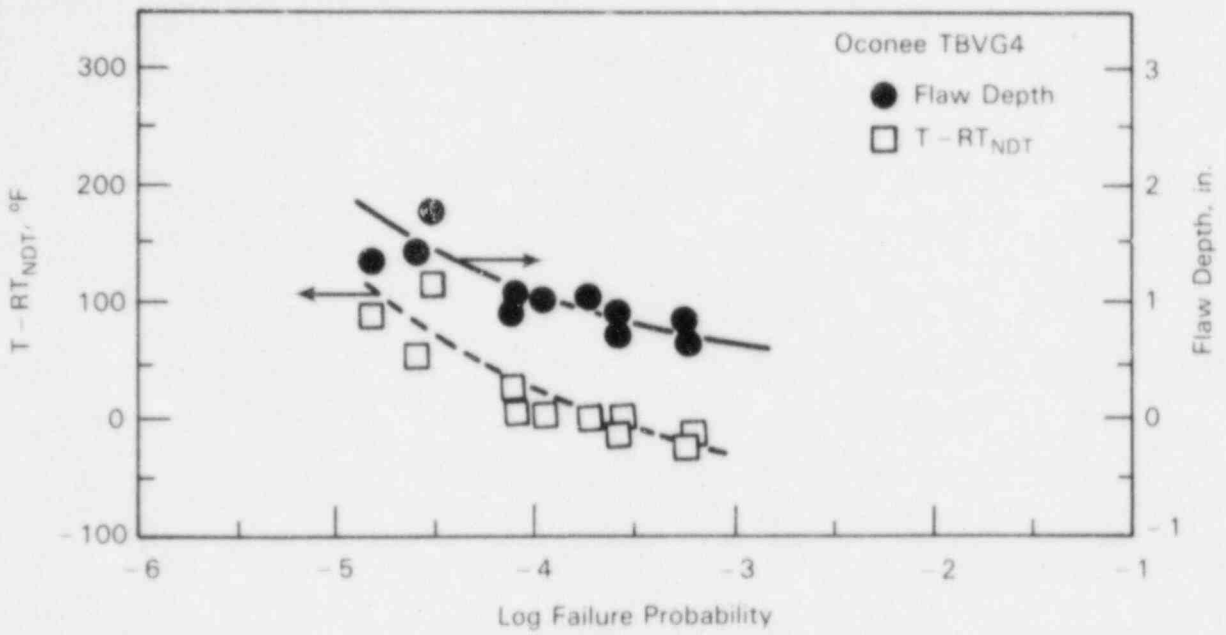

(a)

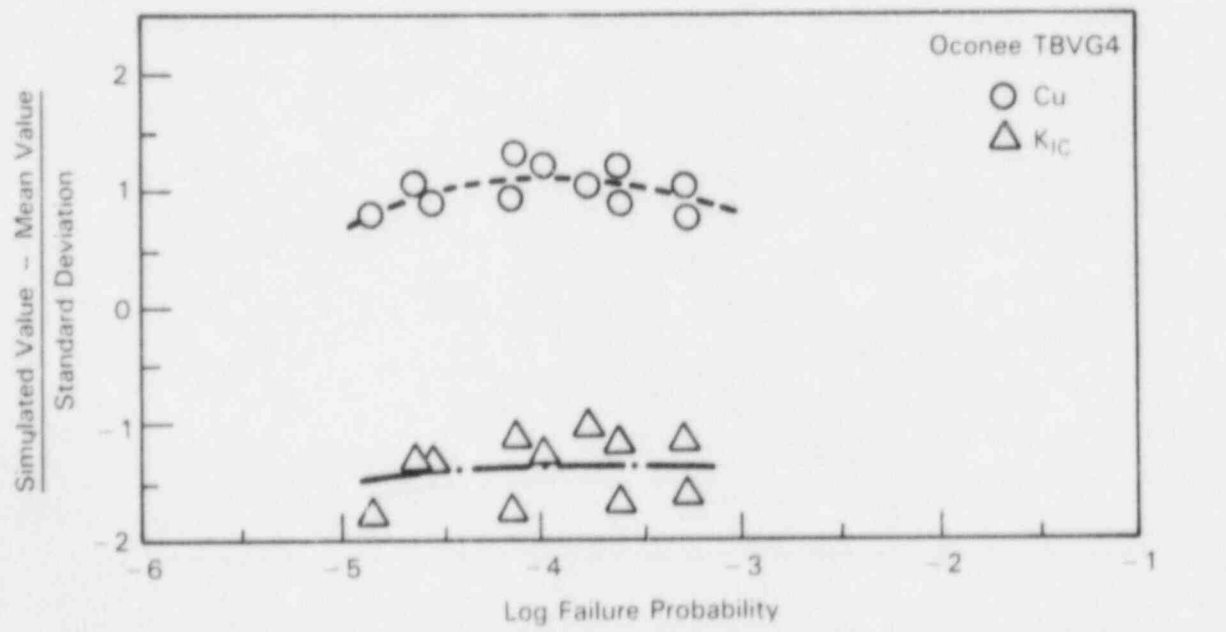

(b)

FIGURE 10. Average simulated parameters for initiation for the Oconee 1 Transient TBVG4. The dependence of simulated flaw depth and the relative temperature, T-RT$_{NDT}$ are shown in (a) and the normalized copper content and fracture toughness are shown in (b). The data plotted are from results of the standard, the copper and the fracture toughness sensitivity cases.

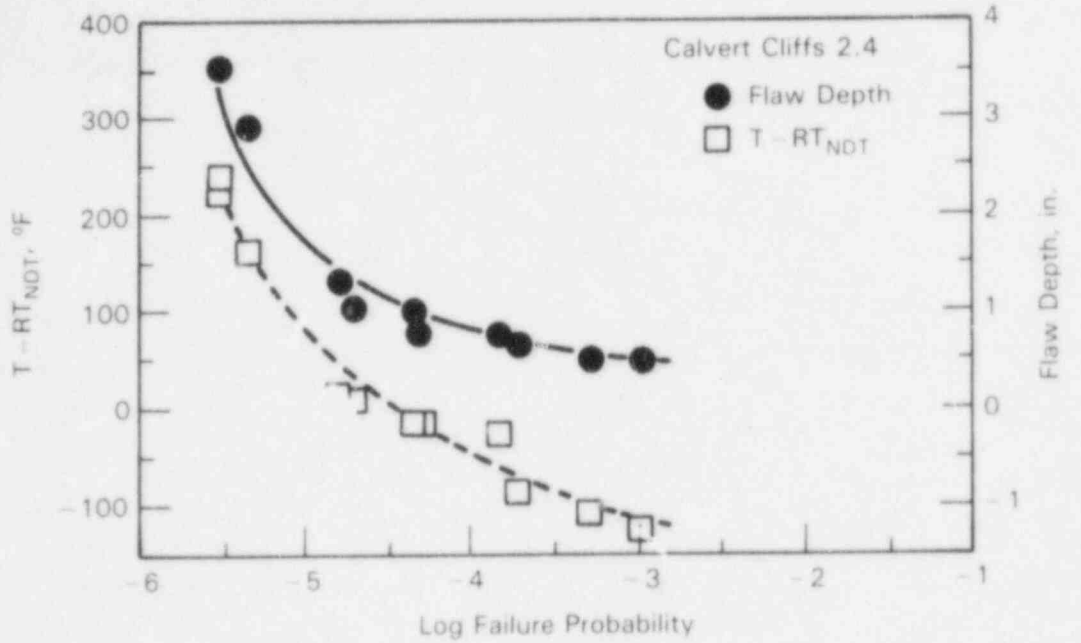

(a)

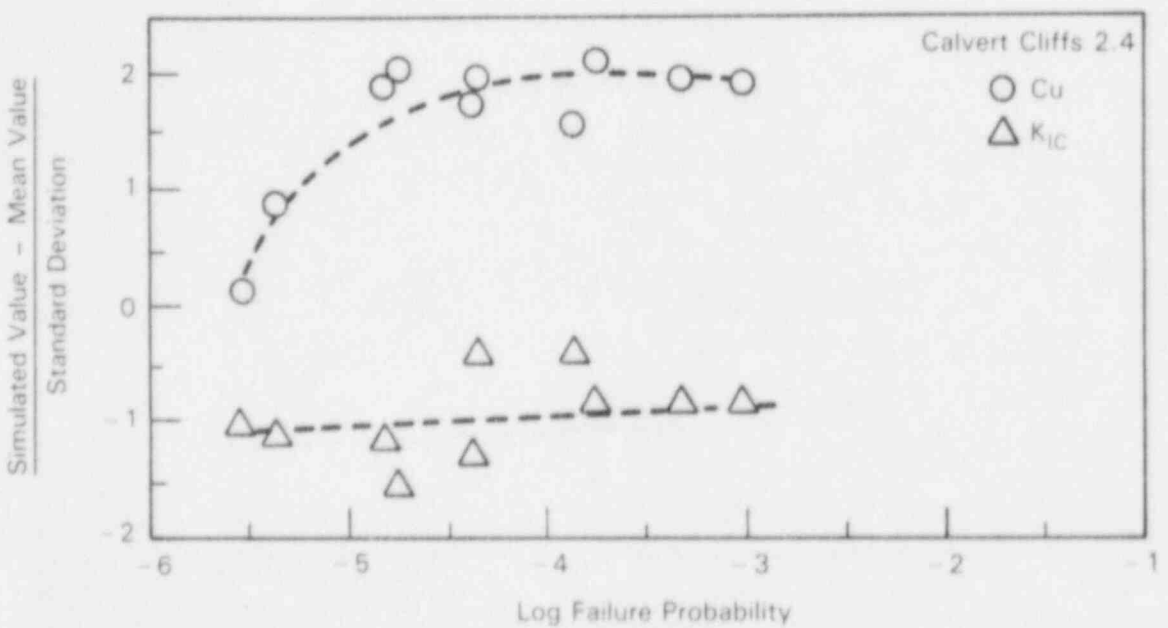

(b)

FIGURE 11. Average simulated parameters for initiation for the Calvert Cliffs 1 Transient 2.4. The dependence of simulated flaw depth and the relative temperature, $T\text{-}RT_{NDT}$, are shown in (a) and the normalized copper content and fracture toughness are shown in (b). The data plotted are from results of the standard, the copper and the fracture toughness sensitivity cases.

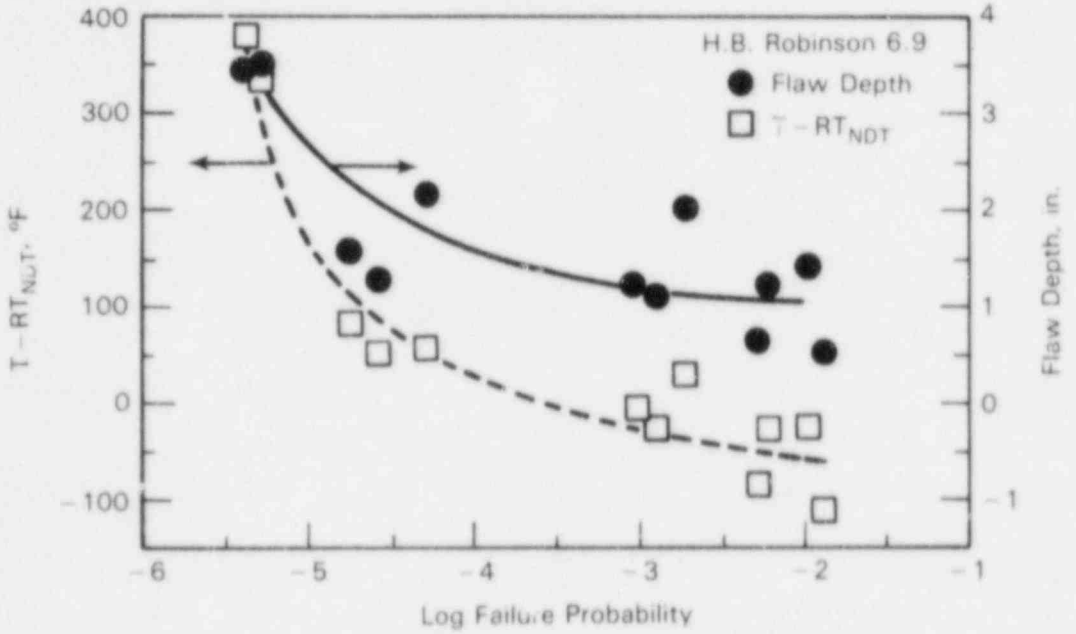

(a)

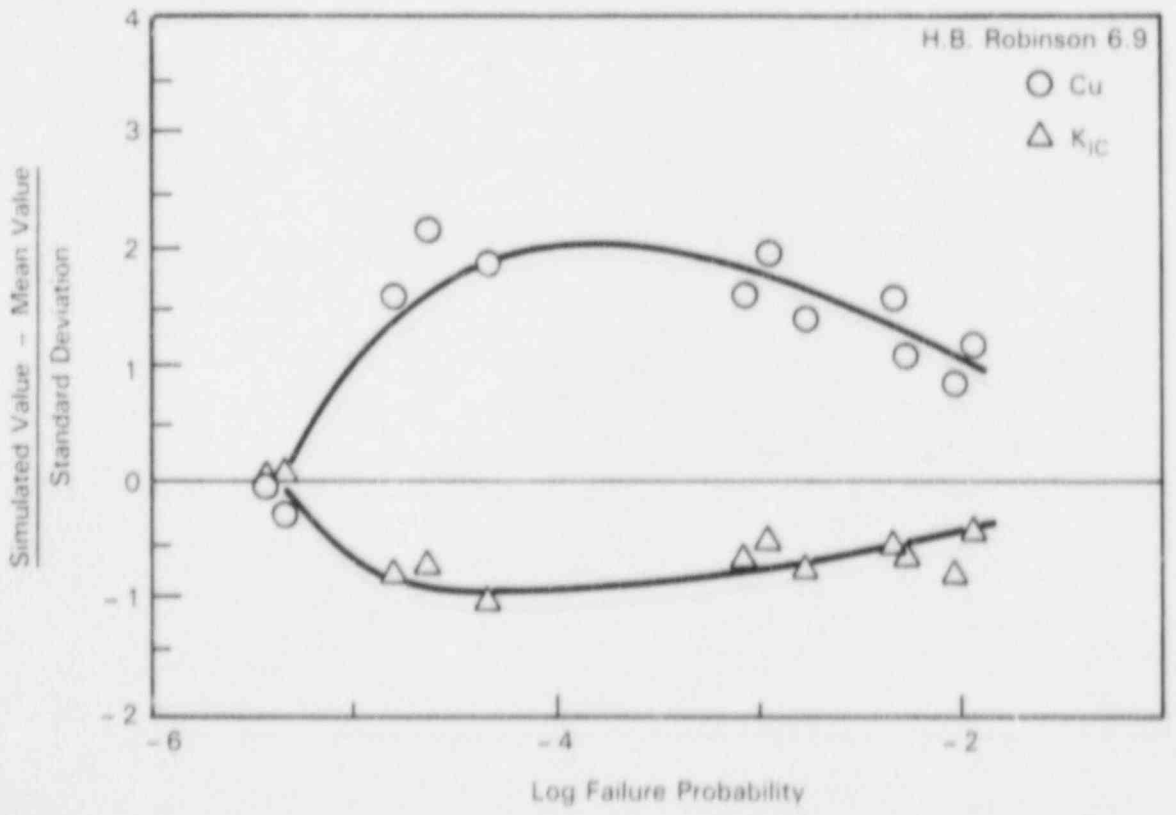

(b)

FIGURE 12. Average simulated parameters for initiation for the hypothetical H. B. Robinson Transient 6.9. The dependence of simulated flaw depth and the relative temperature, $T-RT_{NDT}$, are shown in (a) and the normalized copper content and fracture toughness are shown in (b). The data plotted are from results of the standard, the copper and the fracture toughness sensitivity cases.

TABLE 9. Calculated Failure Probabilities for the Flaw Assumption Sensitivity Study

PLANT TRANSIENT	FLUENCE N/CM**2	CONDITIONAL FAILURE PROBABILITY STD	FINITE FLAW	BURIED FLAW	INSERVICE INSPECTION
OCONEE MSLB1	3.7E+18	2.8E-05	<1.0E-6	1.0E-06	<1.0E-6
	7.0E+18	9.2E-05	<1.0E-6	1.0E-06	4.0E-06
	1.0E+19	5.2E-04	<1.0E-6	5.0E-06	2.4E-05
	1.4E+19	1.4E-03	<1.0E-6	1.9E-05	8.2E-05
OCONEE TBVG4	3.7E+18		<1.0E-6		
	7.0E+18	2.5E-05	<1.0E-6		
	1.0E+19	8.0E-05	<1.0E-6		
	1.4E+19	1.9E-04	<1.0E-6		
OCONEE 6A	3.7E+18	3.0E-05	<1.0E-6	<1.0E-6	<1.0E-6
	7.0E+18	1.1E-04	<1.0E-6	3.0E-06	3.0E-06
	1.0E+19	2.6E-04	1.0E-06	7.0E-06	8.0E-06
	1.4E+19	5.6E-04	8.0E-06	9.0E-06	1.2E-05
CAL CL 8.3	1.9E+19	9.6E-05	1.0E-06	2.0E-06	2.0E-06
	3.8E+19	5.2E-04	6.7E-06	1.0E-05	1.5E-05
	5.7E+19	9.7E-04	2.0E-05	1.8E-05	3.4E-05
	7.6E+19	1.8E-03	8.8E-05	2.7E-05	7.9E-05
	9.5E+19	2.3E-03	1.2E-04	3.8E-05	9.3E-05
HBR 6.6	1.5E+19	9.0E-06	<1.0E-6	<1.0E-6	<1.0E-6
	4.3E+19	1.3E-04	<1.0E-6	2.0E-06	1.0E-06
	9.9E+19	2.5E-03	9.3E-06	2.7E-05	8.9E-05
	2.0E+20	1.3E-02	2.7E-04	9.3E-05	5.0E-04
HBR 6.9	1.5E+19	4.0E-06	<1.0E-6	<1.0E-6	<1.0E-6
	4.3E+19	1.7E-05	<1.0E-6	1.0E-06	<1.0E-6
	9.9E+19	9.1E-04	1.0E-06	3.0E-06	2.0E-05
	2.0E+20	5.8E-03	2.4E-05	5.6E-05	2.0E-04

TABLE 10. Ratios of the Calculated Failure Probabilities for the Flaw Assumption Sensitivity Cases to the Appropriate Standard Cases

PLANT TRANSIENT	FLUENCE N/CM**2	STD FAILURE PROB	SENSITIVITY CASE/STANDARD CASE FINITE FLAW	BURIED FLAW	INSERVICE INSPECTION
OCONEE MSLB1	3.70E+18	2.80E-05		3.60E-02	
	7.00E+18	9.20E-05		1.10E-02	4.40E-02
	1.00E+19	5.20E-04		9.50E-03	4.60E-02
	1.40E+19	1.40E-03		1.30E-02	5.70E-02
OCONEE TBVG4	3.70E+18				
	7.00E+18	2.50E-05			
	1.00E+19	8.00E-05			
	1.40E+19	1.90E-04			
OCONEE 6A	3.70E+18	3.00E-05			
	7.00E+18	1.10E-04		2.70E-02	2.70E-02
	1.00E+19	2.60E-04	3.80E-03	2.70E-02	3.10E-02
	1.40E+19	5.60E-04	1.40E-02	1.60E-02	2.20E-02
CAL CL 8.3	1.90E+19	9.60E-05	1.00E-02	2.00E-02	2.00E-02
	3.80E+19	5.20E-04	1.30E-02	1.90E-02	2.90E-02
	5.70E+19	9.70E-04	2.10E-02	1.90E-02	3.50E-02
	7.60E+19	1.80E-03	5.00E-02	1.50E-02	4.50E-02
	9.50E+19	2.30E-03	4.70E-02	1.50E-02	3.60E-02
HBR 6.6	1.50E+19	9.00E-06			
	4.30E+19	1.30E-04		1.60E-02	7.90E-03
	9.90E+19	2.50E-03	3.70E-03	1.10E-02	3.60E-02
	2.00E+20	1.30E-02	2.10E-02	7.10E-03	3.80E-02
HBR 6.9	1.50E+19	4.00E-06			
	4.30E+19	1.70E-05		5.90E-02	
	9.90E+19	9.10E-04	1.10E-03	3.30E-03	2.20E-02
	2.00E+20	5.80E-03	4.10E-03	9.60E-03	3.50E-02

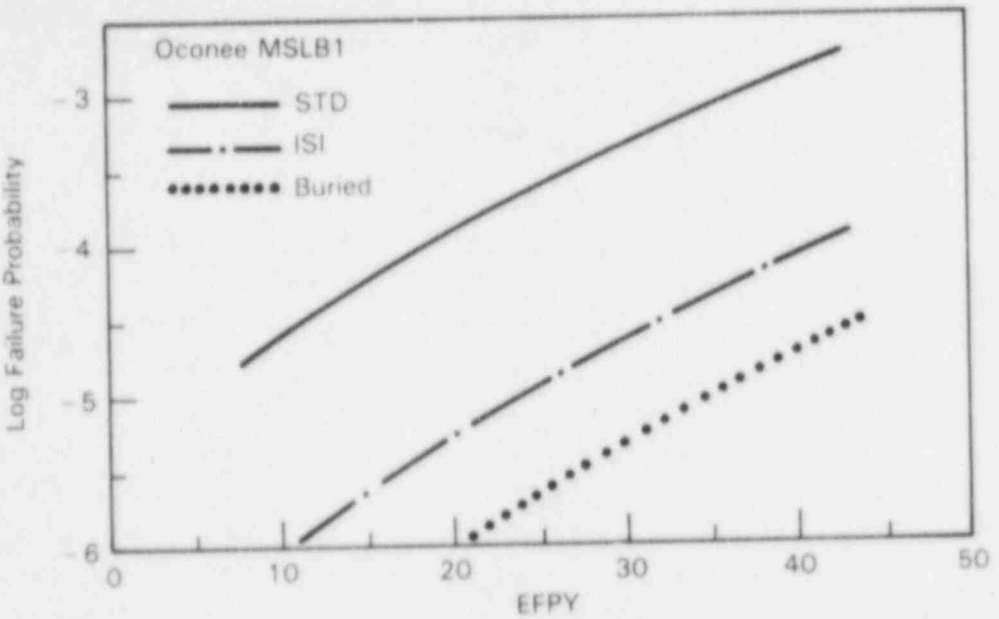

FIGURE 13. Calculated failure probabilities for Oconee 1 Transient MSLB1 for the cases of buried flaws and in-service inspection compared to the standard flaw assumptions

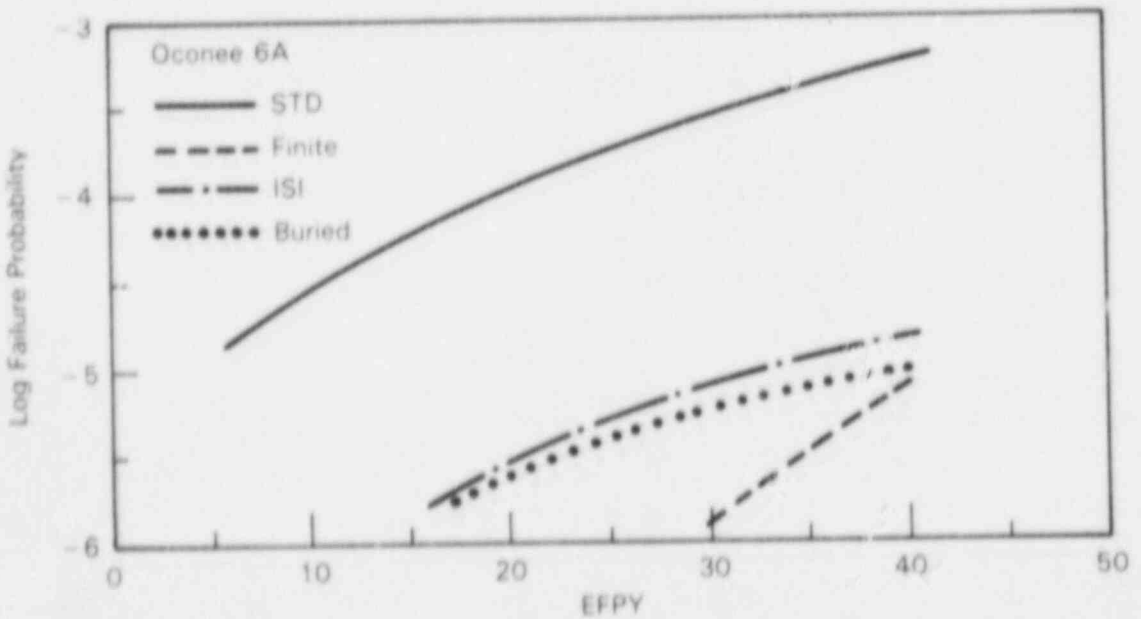

FIGURE 14. Calculated failure probabilities for Oconee 1 Transient 6A for the cases of finite-length flaws, buried flaws, and in-service inspection compared to the standard flaw assumptions

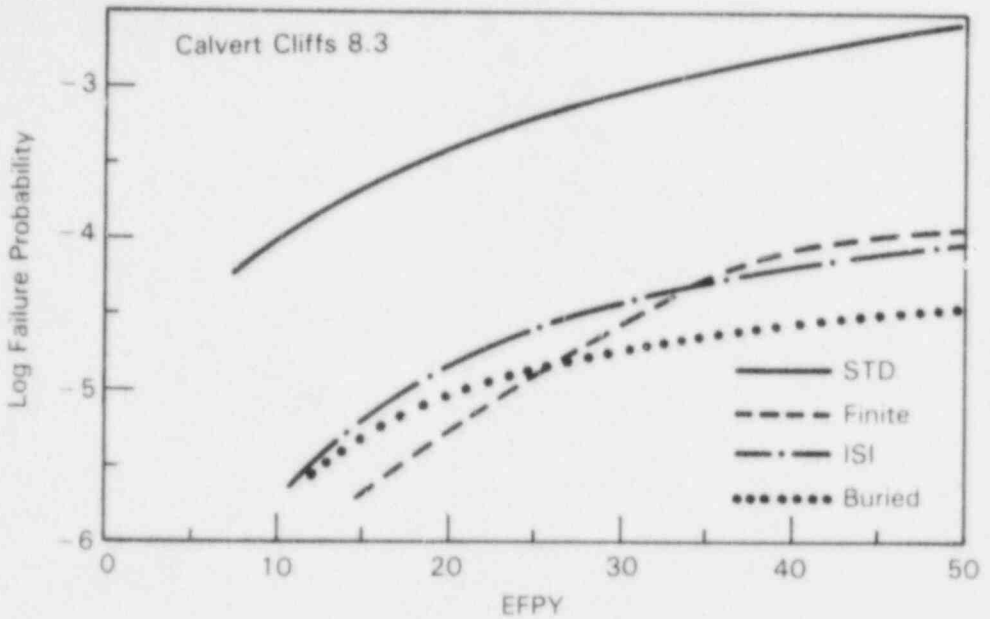

FIGURE 15. Calculated failure probabilities for Calvert Cliffs 1 Transient 8.3 shown for the cases of finite length flaws, buried flaws, and in-service inspection compared to the standard flaw assumptions

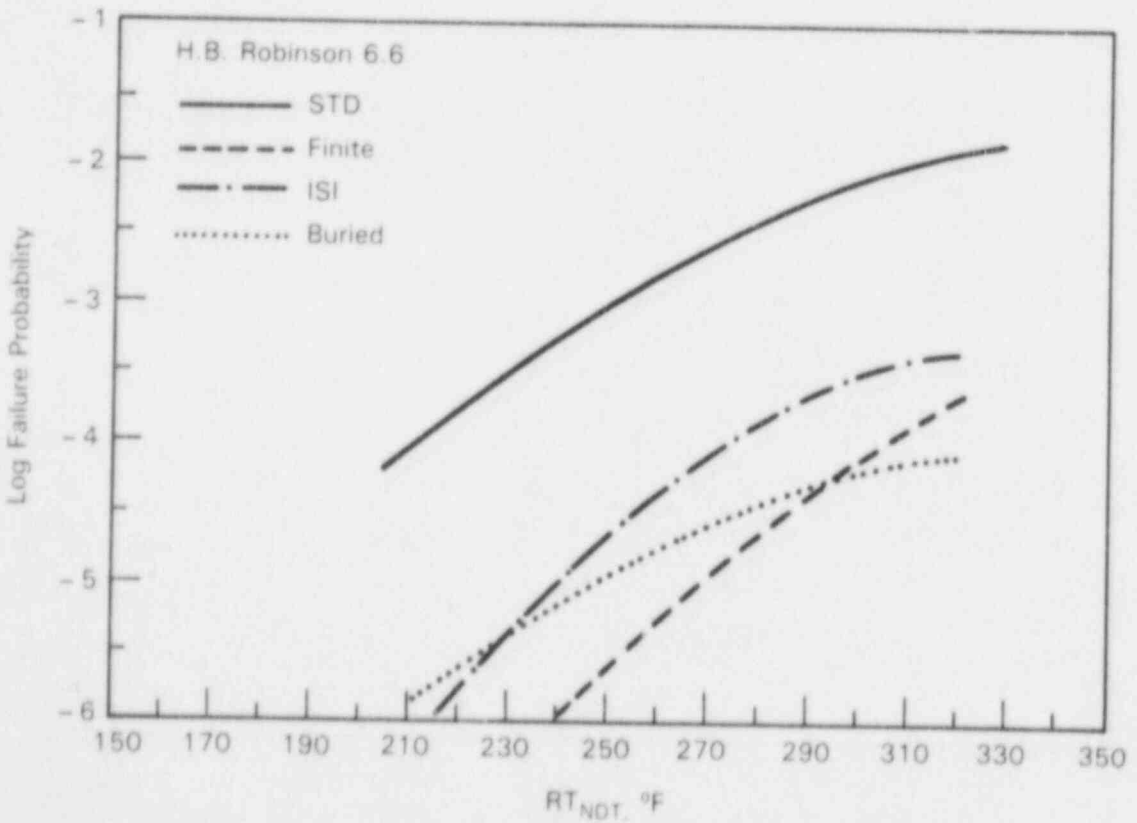

FIGURE 16. Calculated failure probabilities for the hypothetical H. B. Robinson Transient 6.6 for the cases of finite-length flaws, buried flaws, and in-service inspection compared to the standard flaw assumptions

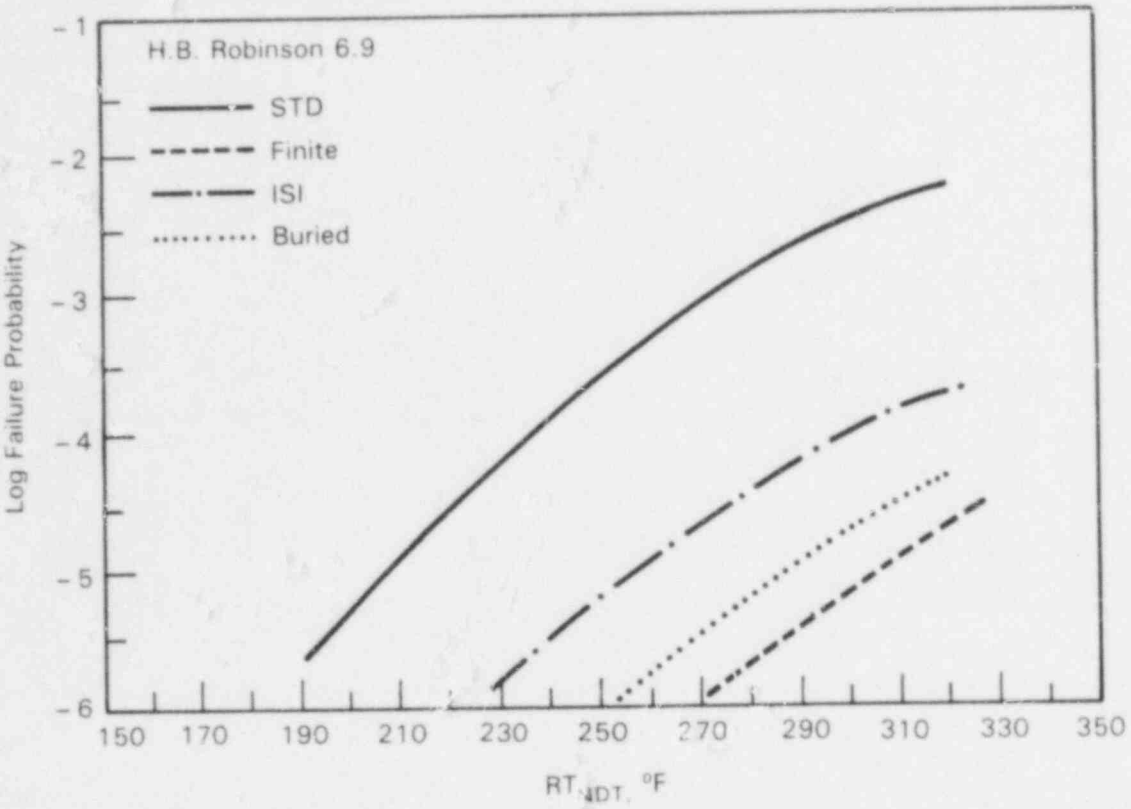

FIGURE 17. Calculated failure probabilities for the hypothetical H. B. Robinson transient 6.9 for the cases of finite length flaws, buried flaws, and in-service inspection compared to the standard flaw assumptions

5.0 CONCLUSIONS AND RECOMMENDATIONS

The effects of material property distributions and flaw assumptions on calculated conditional failure probability were studied. The results demonstrated that flaw uncertainties are more significant than are material property uncertainties. The sensitivities identified in this study indicate recommendations for evaluating methods used for conditional failure probability calculations.

Assumptions concerning flaw characteristics affected the failure probabilities in a critical manner. Therefore, the significance of the calculations has to be evaluated in light of understanding the flaw assumptions made for the calculations. If the calculations are made based on assumptions not commonly accepted, then a sensitivity study is needed to demonstrate the effect of the alternative assumption on the calculated failure probability. A strong effect would suggest that an evaluation of the merits of the alternative assumption should be made. This study has demonstrated that assumptions concerning the length of a flaw, the position of a flaw within the vessel wall, and the effects of in-service inspections and repair are examples of flaw assumptions that need to be evaluated in sensitivity studies. These flaw assumptions were found to have significant effects for all cases examined and therefore are expected to be important for most pressurized thermal shock analyses. However, lacking strong justification, the flaws should conservatively be assumed to be infinitely long, at the surface, and not inspected.

The effect of material property uncertainties on calculated failure probabilities was less important than were the effects of flaw assumptions. Also, material property distributions are better established than are flaw distributions. Therefore, plant-specific knowledge of materials can be used in calculations to provide a more realistic estimate of expected failure probability. The uncertainties in copper content, nickel content, and fracture toughness in this study were both realistically small for specific welds and realistically large for generic welds. The difference between results for the small specific uncertainty and the large generic uncertainty generally did not have dominant effects on the calculated failure probabilities.

The uncertainty in copper content sensitivity had a strong effect only for failure probabilities that were less than 10^{-4}. Such low failure probabilities are not of practical interest to PTS risk. The copper content uncertainty is not expected to affect the calculated failure probability by more than a factor of three for PTS conditions that produce predicted failure probabilities greater than 10^{-4}.

The nickel content uncertainty generally had an insignificant effect on the calculated failure probabilities and therefore need not be included in a failure probability study. The only significant effects of nickel content uncertainty occurred for conditions that resulted in insignificant failure probabilities that were lower than 10^{-4}.

Increasing the uncertainty (standard deviation) in the fracture toughness from 10% to 20% of the assumed mean value increased the predicted failure

probability by a factor of less than five. A 10% uncertainty in toughness is a realistic estimate for failures approaching the lower shelf on the fracture toughness-versus-temperature plot, at which conditions the predicted failure probabilities are relatively high, i.e., greater than 10^{-4}. For these conditions, there is a lack of justification for selecting the larger, 20% uncertainty. At conditions of lower failure probability, a larger uncertainty might be justified because the fracture toughness is being estimated in the transition region between brittle and ductile failure.

The fracture toughness is less well established in the transition region and therefore a larger, 20%, uncertainty might be justified. However, because the failure probabilities are low in the transition region and because the fracture toughness sensitivity is small, the assumption of a 10% uncertainty in fracture toughness is considered to be appropriate.

Adding an error simulation to account for uncertainty in the trend curve correlation did not significantly affect the predicted failure probability compared to not simulating the correlation error. Because the effect was found to be small, the correlation error need not be included in the prediction of failure probability.

The analyses of simulated values for initiation events indicated that the extreme tails of the material property distributions were not significantly influencing the predicted failure probabilities. The predicted failures were typically caused by simulated values that were within two standard deviations of the assumed mean values. Therefore, the input distributions for the material property estimates need only be understood out to about two standard deviations from the mean values. The copper content distribution and the fracture toughness distribution are experimentally established within the two-sigma range and therefore are appropriate distributions to use.

The analyses of the average flaw depth and the average $T\text{-}RT_{NDT}$ for initiations indicated that there is a transition in fracture mode from ductile failure of deep flaws at low failure probabilities to brittle failure of shallow flaws at high failure probabilities. This transition should be considered when examining the relative importance of material property input distributions on predicted failure probabilities. For example, the copper content distribution was found to have its greatest effect at intermediate failure probabilities because of the influence of copper on the brittle and ductile failure modes. Uncertainty in the fracture toughness distribution becomes more important at lower failure probabilities because the failures become independent of the irradiation induced properties and more dependent on the unirradiated properties.

REFERENCES

1. D. L. Stevens et al. 1983. VISA - A Computer Code for Predicting the Probability of Reactor Pressure Vessel Failure. NUREG/CR-3384 (PNL 4774), prepared for the U.S. Nuclear Regulatory Commission by Pacific Northwest Laboratory, Richland, Washington.

2. R. D. Cheverton and D. G. Ball. 1984. OCA-P, A Deterministic and Probabilistic Fracture-Mechanics Code for Application to Pressure Vessels. NUREG/CR-3618 (ORNL-5991), prepared for the U. S. Nuclear Regulatory Commission by Oak Ridge National Laboratory, Oak Ridge, Tennessee.

3. T. J. Burns et al. 1984. Pressurized Thermal Shock Evaluation of the Oconee-1 Nuclear Power Plant. NUREG/CR-3770 (ORNL/TM-9176), prepared for the U. S. Nuclear Regulatory Commission by Oak Ridge National Laboratory, Oak Ridge, Tennessee.

4. D. L. Selby et al. 1984. Pressurized Thermal Shock Evaluation of the Calvert Cliffs Unit 1 Nuclear Power Plant. NUREG/CR-4022 (ORNL/TM-9408), prepared for the U. S. Nuclear Regulatory Commission by Oak Ridge National Laboratory, Oak Ridge, Tennessee.

5. D. L. Selby et al. 1985. Pressurized Thermal Shock Evaluation of the H. B. Robinson Unit 2 Nuclear Power Plant. NUREG/CR-4183. (ORNL/TM-9567), prepared for the U.S. Nuclear Regulatory Commission by Oak Ridge National Laboratoiry, Oak Ridge, Tennessee.

6. Policy Issue from J. W. Dircks to NRC Commissioners. "Enclosure A: NRC Staff Evaluation of Pressurized Thermal Schock, November 1982." SECY-82-465, November 23, 1982. Division of Nuclear Reactor Regulation, U.S. Nuclear Regulatory Commission, Washington, D.C.

7. K. E. Moore and A. S. Heller. 1983. B&W 177-FA Reactor Vessel Beltline Weld Chemistry Study. BAW-1799, prepared for Westinghouse Electric Company by Babcock and Wilcox, Lynchburg, Virginia.

8. Combustion Engineering, Inc. 1981. Evaluation of Pressurized Thermal Shock Effects Due to Small Break LOCA's with Loss of Feedwater for the Combustion Engineering NSSS. CEN-189, Windsor, Connecticut.

9. W. N. McElroy, A. I. Davis, and R. Gold. 1981. Surveillance Dosimetry of Operating Power Plants. HEDL-SA-2546, Hanford Engineering Development Laboratory, Richland, Washington.

10. G. L. Guthrie and W. N. McElroy. 1982. LWR Pressure Vessel Surveillance Dosimetry Improvement Program: Quarterly Progress Report January 1982-March 1982. NUREG/CR-2805, Volume 1, (HEDL-TME 82-18), Hanford Engineering Development Laboratory, Richland, Washington.

11. G. R. Odette and P. Lombrozo. 1983. "A Physically Statistically Based Correlation for Transition Temperature Shifts in Pressure Vessel Steel Surveillance Welds." Trans. Am. Nuc. Soc. 44:224.

12. E. P. Lippincott and W. N. McElroy. 1983. LWR Pressure Vessel Surveillance Dosimetry Improvement Program: Quarterly Progress Report October 1982-December 1982, NUREG/CR-2805, Volume 4, (HEDL-TME 18-21), Hanford Engineering Development Laboratory, Richland, Washington.

13. W. Marshall. 1976. An Assessment of the Integrity of PWR Pressure Vessels. Study Group Report, Services Branch, United Kingdom Atomic Energy Agency, London.

14. W. E. Vesely, E. K. Lynn, and F. F. Goldberg. 1978. The Octavia Computer Code: PWR Reactor Pressure Vessel Failure Probabilities Due to Operationally Caused Pressure Transients. NUREG-0258, U.S. Nuclear Regulatory Commission, Washington, D.C.

15. T. T. Taylor, S. R. Crawford, S. R. Doctor, and G. J. Posakony. 1983. Detection of Small-Sized Near-Surface Under-Clad Cracks for Reactor Pressure Vessels. NUREG/CR-2878, Nuclear Regulatory Commission, Washington, D.C.

NUREG/CR-4267
PNL-5469

DISTRIBUTION

No. of Copies

OFFSITE

U.S. Nuclear Regulatory Commission
Division of Technical Information
and Document Control
7920 Norfolk Avenue
Bethesda, MD 20014

15 R. Woods
Division of Safety Technology
Nuclear Reactor Regulation
Nuclear Regulatory Commission
Washington, D.C. 20555

15 M. Vagins
Division of Engineering Technology
Office of Nuclear Regulatory Research
Nuclear Regulatory Commission
Washington, D.C. 20555

No. of Copies

ONSITE

42 Pacific Northwest Laboratory

W. J. Apley
M. C. Bampton
C. A. Bennett (HARC)
S. H. Bian
E. L. Courtright
D. W. Engel
C. R. Hann
K. I. Johnson
W. W. Laity
J. A. Mahaffey
L. T. Pedersen
P. J. Pelto
G. J. Posakony
R. E. Rhoads
E. P. Simonen (10)
F. A. Simonen (5)
A. M. Sutey
T. T. Taylor
D. S. Trent
P. L. Whiting
R. D. Widrig
L. D. Williams
Publishing Coordination (2)
Technical Information (5)

NRC FORM 335 (2-84) NRCM 1102, 3201, 3202

U.S. NUCLEAR REGULATORY COMMISSION

BIBLIOGRAPHIC DATA SHEET

SEE INSTRUCTIONS ON THE REVERSE

1. REPORT NUMBER (Assigned by TIDC, add Vol. No., if any)
NUREG/CR-4267
PNL-5469

2. TITLE AND SUBTITLE
VESSEL INTEGRITY SIMULATION (VISA) CODE SENSITIVITY STUDY

3. LEAVE BLANK

4. DATE REPORT COMPLETED
MONTH: June YEAR: 1985

5. AUTHOR(S)
E.P. Simonen
K.I. Johnson
F.A. Simonen

6. DATE REPORT ISSUED
MONTH: December YEAR: 1985

7. PERFORMING ORGANIZATION NAME AND MAILING ADDRESS (Include Zip Code)
Pacific Northwest Laboratory
P.O. Box 999
Richland, Washington 99352

8. PROJECT/TASK/WORK UNIT NUMBER

9. FIN OR GRANT NUMBER
B2510

10. SPONSORING ORGANIZATION NAME AND MAILING ADDRESS (Include Zip Code)
Division of Safety Technology
Office of Nuclear Reactor Regulation
U.S. Nuclear Regulatory Commission
Washington, DC 20555

11a. TYPE OF REPORT
Topical

b. PERIOD COVERED (Inclusive dates)

12. SUPPLEMENTARY NOTES

13. ABSTRACT (200 words or less)

In a study conducted for the Nuclear Regulatory Commission by Pacific Northwest Laboratory, the sensitivity of through-wall crack probability to input distributions was studied. Flaw growth characteristics were evaluated for three pressurized water reactor plants (Oconee 1, Calvert Cliffs 1, and a hypothetical plant similar to H. B. Robinson 2). Three postulated pressurized thermal shock (PTS) transients were considered for each plant. This report describes the results of material and flaw distribution assumptions on calculated conditional failure probabilities for the three reactors under postulated severe PTS transients. The reasons for the predicted sensitivities are evaluated and are related to requirements for defining input distributions for probabilistic failure predictions.

14. DOCUMENT ANALYSIS – a. KEYWORDS/DESCRIPTORS
Pressurized water reactor
Pressurized thermal shock
VISA code

b. IDENTIFIERS/OPEN-ENDED TERMS

15. AVAILABILITY STATEMENT
Unlimited

16. SECURITY CLASSIFICATION
(This page) Unclassified
(This report) Unclassified

17. NUMBER OF PAGES

18. PRICE

NUREG/CR-4267

VESSEL INTEGRITY SIMULATION ANALYSIS (VISA) CODE SENSITIVITY STUDY

DECEMBER 1985